AN ABSTRACT OF THE THESIS OF

Adam B. Mazurkiewicz for the degree of Masters of Science in Forest Engineering presented on September 19, 2006.
Title: Measurement and Modeling the Physical Controls of Snowmelt in the Pacific Northwest

Abstract approved:

_____

Jeffrey J. McDonnell

The physical controls of snowmelt in the Pacific Northwest (PNW) are poorly understood. While there have been numerous field and modeling investigations at the plot and watershed scale, few studies have identified how the snow energy balance (EB) components vary in importance both spatially and temporally. The identification of how dominant EB components vary in space and time will allow us to understand how the snow regime will be affected by environmental change. We apply two physically based snow energy balance models (SNOBAL and ISNOBAL) to two different climate regimes of PNW Cascade Mountains to investigate the spatial and temporal variability of EB components which cause snowmelt. We found that radiation dominated the EB in both the rain-on-snow, Western Cascades environment and in a semi-arid watershed in the Eastern Cascades. Turbulent energy exchanges varied with topographic position, vegetation, and most importantly wind speed. In both modeling scenarios warmer winters led to shallower snowpack accumulation. Shorter snow seasons resulted in lower radiation inputs and higher sensible heat exchanges in the annual EB. Numerical simulation of snowmelt processes has helped

to provide an understanding of the anticipated effects of environmental change on the snow regime in the PNW.

Measurement and Modeling the Physical Controls of Snowmelt in the Pacific Northwest

by
Adam B. Mazurkiewicz

A THESIS

submitted to

Oregon State University

in partial fulfillment of
the requirements for the
degree of

Master of Science

Presented September 19, 2006
Commencement June 2007

Master of Science thesis of Adam B. Mazurkiewicz
presented on September 19, 2006

APPROVED:

_____

Major Professor, representing Forest Engineering

_____

Head of the Department of Forest Engineering

_____

Dean of the Graduate School

I understand that my thesis will become part of the permanent collection of the Oregon State University libraries. My signature below authorizes release of my thesis to any reader upon request.

_____

Adam B. Mazurkiewicz, Author

ACKNOWLEDGEMENTS

I am most grateful to my constant companion in life, sailing, and skiing, Brooke. Without her tolerance for high winds, Cascade powder, long work days, and my bad attitude, I would be a lonely guy. I would also like to thank my parents for their years of loving support in all my endeavors.

I cannot thank my advisor Jeff McDonnell enough. He has led me down a dark path, which does have light at the end. His constant passion for research and science gave me the motivation to endure the pains of modeling. I am truly grateful for all his guidance and motivation.

I would also like to thank everyone on the Oregon Snow Survey Staff — Bill Overman, Melissa Webb, Sheila Strachan, Jon Lea, Scott Pattee, and Rashawn Tama-Sweet — who have contributed endless hours of support during my snow hydrology career. Working with this group gave me the skills to accomplish my goals. I especially thank Melissa Webb for her help installing snow pillows in the Entiat. I also cannot thank Bill Overman enough for the years of guidance in the field.

I am deeply indebted to David Garen for all of his guidance in the modeling world. Without his handholding and gentle tone, I would be old and gray. I would also like to thank Danny Marks who motivated me to take on a modeling-based thesis. The modeling conversations I have had with Nicolai Thum, Kellie Vache, and Mario Martina helped me to get started on the long path of model results.

I would also like to thank my committee members Rick Woodsmith, Anne Nolin, and Jack Istok. I especially thank Rick Woodsmith for providing data and field support.

A very special thanks to the Hillslope Hydrology Group — Chris Graham, Willem van Verseveld, David Alley, David Callery, Holly Barnard, Kellie Vache, Jeff McDonnell, and April James. I consider myself extremely fortunate to have had the opportunity to work and socialize with such a motivated and fun group. I especially thank David Callery for his contributions and discussions about the HJA. I also thank David Alley who put forth great efforts in the field.

Last but not least, I need to thank the various crew of *'Eve'* — Brooke, Holly, Chris, Dave, April, Jeff, Denise, John — Thursdays make the week and we have come a long way. Financial support for my graduate program was provided by the USDA – Forest Service through the contract PNW 03-CA-11261921-529 - *Processes of Water Cycling and Streamflow Generation in Semi-Arid Watersheds in Eastern Washington-Understanding Landuse Effects on Water Quantity and Quality.*

CONTRIBUTIONS OF AUTHORS

Chapter 1: David Callery assisted with analysis of modeling results and editing. Jeff McDonnell provided writing guidance and editing.

Chapter 2: Jeff McDonnell provided data interpretation and critical manuscript reviews. David Garen provided guidance in developing model forcing data. Danny Marks provided model assistance. Rick Woodsmith provided field data.

TABLE OF CONTENTS

TABLE OF CONTENTS (Continued)

LIST OF FIGURES

LIST OF TABLES

1 INTRODUCTION

1.1 INTRODUCTION

The physical controls of snowmelt in the Pacific Northwest (PNW) are poorly understood. In particular, the temporal and spatial variability of snow energy balance (EB) components that drive snowmelt and how they vary on either side of the Cascade Mountains is not well characterized. A thorough understanding of these components is needed to help estimate the timing and peak of snowmelt for planning water resource management projects and quantifying the response to land use and climate change. Increased social pressures on water resources have generated new questions about the PNW snow regime. Changes in land cover (VanShaar et. al., 2002) and variability in annual average air temperature will affect snow accumulation and melt patterns (Mote, 2003; Serreze, 1999). The absence of forest canopy has been shown to increase snow accumulation from 5-70% (Golding and Swanson, 1986; Troendle et. al. 1988; Winkler et. al., 2005). A change in the near-surface air temperature regimes has led to decreasing mountain snowpacks in the PNW (Mote, 2003; Service, 2004). These observations demand predictions to investigate the controls of snowmelt in the PNW and identify how accumulation will change spatially and temporally in response to environmental change.

The development of new tools such as physically-based snow energy and mass balance models has allowed snow hydrology to begin to address new questions in the changing environment. Physically-based snow energy balance models have allowed investigations to decipher how snow accumulation and melt varies across complex terrain (Marks and Winstral, 2001; Link and Marks, 1999; Garen and Marks, 2005). Since the modeling schemes have been shown to reproduce measured conditions,

these models can now be used to explore scenarios of environmental change and to identify the potential results of a changing environment. Weiler and McDonnell (2004) suggested the use of 'numerical experiments with a model driven by collective field intelligence' as a learning tool to investigate a changing environment. The established routines to model snow cover allow us to explore the EB components during environmental change scenarios. This thesis applies this philosophy to quantify spatial and temporal changes in EB components and to identify their influence in creating snowmelt under environmental change, at the point and watershed scale.

We focus our investigation on the PNW, U.S.A. The PNW, like many other mountainous regions, relies on the snowpack as a storage reservoir of water (Serreze, 1999). The region has a diverse climate, ranging from temperate rainforest conditions on the western side of the Cascade Mountains to high desert conditions on the eastern side of the Cascades. This has caused an often simplified description of two melt regimes for the region, divided by the Cascade Mountain Crest. The snow regime on the west-side of the Cascade Mountains is typically thought of as a turbulent exchange dominated due to the number of studies which have focused on deciphering processes which cause snowmelt during rain-on-snow (ROS) events (Berris and Harr, 1987; Harr, 1981; Marks et. al. 1998). These studies have shown that the combination of warm air temperatures and high humidity coupled with high wind speeds results in increased turbulent energy exchanges of sensible and latent heat, which can dominant the EB during major ROS events (Marks et. al., 1998). The snow regime of the east-

side of the Cascade Mountain crest is poorly described, but due to the typically dry conditions, is assumed to be dominated by radiation.

1.2 DESCRIPTION OF CHAPTERS

1.2.1 Chapter 1. Physical controls on snowmelt in a rain-on-snow environment

Chapter 1 uses a point scale snow energy and mass balance model (SNOBAL) to investigate the variability of EB controls in the H.J. Andrews Experimental Forest (HJA). This experimental watershed is located on the west slope of the Oregon Cascade Mountains. The snow regime has been characterized as a rain-on-snow environment. We applied SNOBAL to an eight year dataset at three climate stations, to decipher the dominant components of the EB which control melt. The long term dataset at three climate stations, which traverses the transient to the seasonal snow zone, make this a novel approach in identifying the dominant snowmelt controls. The main questions addressed in this portion of the research are:

1. What are the EB components of snowmelt at HJA on an annual time scale?
2. How does their relative importance change with different time scales?
3. What are the dominant components of the EB during high-frequency ROS events?
4. How much annual snowmelt comes from ROS events vs. non-ROS event melt?
5. How do energy balance components vary by site elevation, exposure, aspect?

1.2.2 Chapter 2. The effect of environmental change on watershed-scale snow regime: a virtual experiment approach

The influence of environmental change on the snow regime is the focus of chapter 2. We apply a spatially distributed snow energy and mass balance model (ISNOBAL) to identify the controls of snowmelt in a 580 ha watershed, located on the east-slope of the Washington Cascades, U.S.A., for the water year 2006. We then use ISNOBAL to simulate environmental change scenarios to investigate the potential changes in EB inputs to melt both temporally and spatially. The main objectives in this chapter are:

1. Reproduce the observed snowmelt patterns.
2. Identify the main energy balance components of snowmelt and describe how the components vary within space and time throughout the melt season.
3. Determine the relative melt contribution of each EB component.
4. Evaluate the effects of increases in average air temperature and land cover change to evaluate the changes on EB components.

1.3 REMARKS

Chapter 1 data were available through the HJA webpage, while data in chapter 2 were acquired through the existing meteorological network established in the Entiat Experimental Forest. In addition to the climate stations, two snow pillow sites were installed to validate snow model simulations. Each station was instrumented with two steel snow pillows and air temperature sensors. Field visits were made to make snow course measurements and to maintain and download station data.

1.4 REFERENCES

Berris, S., Harr, R.D., 1987. Comparative snow accumulation and melt during rainfall in forested and clear-cut plots in the western Cascades of Oregon. Water Resources Research 23, 135-142.

Garen, D. Marks, D., 2005. Spatially distributed energy balance snowmelt modeling in a mountainous river basin: Estimation of meteorological inputs and verification of model results. Journal of Hydrology 315, 126-153.

Golding, D.L., Swanson, R.H., 1986. Snow distribution patterns in clearings and adjacent forest. Water Resources Research 22, 1931-1940

Harr, R.D., 1981. Some characteristics and consequences of snowmelt during rainfall in Western Oregon. Journal of Hydrology 53. 277-304.

Link, T., Marks, D., 1999. Distributed simulation of snowcover mass- and energy-balance in the Boreal forest. Hydrological Processes 13, 2439-2452.

Marks, D., Winstral, A., 2001. Comparison of snow deposition, the snow cover energy balance, and snowmelt at two sites in a semiarid mountain basin. Journal of Hydrometeorology 2, 213-227.

Marks, D., Kimball, J., Tingey, D., Link, T., 1998. The sensitivity of snowmelt processes to climate conditions and forest cover during rain-on-snow: A case study of the 1996 Pacific Northwest flood. Hydrological Processes 12, 1569-1587.

Meiman, J.R., 1987. Influence of forests on snowpack accumulation. Management of subapline forests: Building on 50 yrs of Research. USDA Forest Service, Rocky Mountain Forest and Range Esperiment Station. General technical report RM-149.

Mote, P.W., 2003. Trends in snow water equivalent in the Pacific Northwest and their climatic causes. Geophysical Research Letters 30(12), 1-4.

Serreze, M.C., Clark, M.P., Armstrong, R.L., McGinnis, D.A., Pulwarty, R.S., 1999. Characteristics of the western United States snowpack from snowpack telemetry (SNOTEL) data. Water Resources Research 35(7), 2145-2160.

Service, R.F., 2004. As the west goes dry. Science Magazine 303, 1124-1127.

Troendle, C.A., Schmidt, R.A., Martinez, M.H., 1988. Snow deposition processes in a forest stand with a clearing. In the Proceedings of the 56th Western Snow Conference, 78-86.

Weiler, M., McDonnell, J., 2004. Virtual Experiments: a new approach for improving process conceptualization in hillslope hydrology. Journal of Hydrology 285, 3-18.

Winkler, R.D., Spittlehouse, D.L., Golding, D.L., 2005. Measured differences in snow accumulation and melt among clearcut, juvenile, and mature forests in southern British Columbia. Hydrological Processes 19, 51-62.

VanShaar, J.R., Haddeland, I., Lettenmaier, D.P., 2002. Effects of land-cover changes on the hydrological response of interior Columbia basin forested catchments. Hydrological Processes 16, 2499-2520.

2 Physical controls on snowmelt in a rain-on-snow environment

Mazurkiewicz, A.B.

Callery, D.G.

McDonnell, J.J.

To be submitted to:

Journal of Hydrology
Elsevier Inc., Amsterdam, Netherlands
in preparation

2.1 INTRODUCTION

Rain-on-snow (ROS) events are a common driver of flooding in many temperate regions. In the Pacific Northwest (PNW) of the USA, ROS events are synonymous with the largest flooding events. Harr (1981) noted that 21 of the top 23 highest annual peak flows of the Willamette River at Salem, Oregon between 1814 and 1977 were associated with ROS. These events are often a combination of high melt rates in low elevation snowpack driven by turbulent energy exchange (Marks et. al., 1998), accumulated rainfall, and high antecedent soil moisture conditions which cause stream flows to rapidly rise. The importance of these events in creating peak stream discharges and flooding has made ROS a focal point of snow hydrology studies in the PNW (Berris and Harr, 1987; Harr, 1981; Marks et. al., 1998).

Experimental analysis (Berris and Harr, 1987) of PNW ROS events and more recent model analysis of the same dataset (van Heeswiijk et al., 1996) show that rainfall rates alone have little effect on the production of snowmelt. van Heeswijk et al. (1996) showed that doubling precipitation added only 0.1 – 0.5 mm snowmelt for the three events recorded by Berris and Harr (1987), while adding 2°C to the air temperature increased snowmelt by 0.7 – 5.8 mm. They concluded that the generation of snowmelt during ROS is most sensitive to wind speed, but is also responsive to high humidity and temperature gradients if they occur in conjunction with high wind speeds.

Due to the protracted rainfall regime of PNW winters and the hydrological importance of snowmelt during rainfall, snowmelt in the PNW is often characterized as turbulent exchange dominated. Notwithstanding, very few experimental studies

have actually focused on energy balance (EB) dynamics of melting snow in the PNW. The most extensive such work was conducted at the Willamette Basin Snow Laboratory (WBSL) in the Blue River Watershed during the period 1947-1952 (U.S.A.C.E., 1956). This project led to the development of general snowmelt equations and thermal budget indices. Berris and Harr (1987), working at the H.J. Andrews Experimental Forest (HJA) in the western Cascade Mountains of Oregon found that snowmelt in forested sites during ROS events were much lower than in open sites in the transient snow zone. Absence of trees resulted in continuous higher energy balance inputs to the snowpack creating a consistently isothermal snowpack. Marks et. al. (1998) found 60-90% of snowmelt was driven by turbulent energy exchanges during one of the largest recorded ROS events in the region which occurred in February 1996.

In spite of these detailed studies, there is limited data covering different times of the melt season and at different elevations to underpin the general notion of turbulent flux domination of the snow energy balance regime in the PNW. Despite this, the conception of a ROS-dominated melt regime in the PNW persists. Hydrology studies focused on streamflow data often cite ROS events as the main driver of peak discharges and geomorphologic processes, e.g. "increases in ROS peak discharges after forest canopy removal are greater in basins with large snowpacks" (Jones and Swanson, 2001, pg. 2365). While these studies provide a depiction of streamflow generation in the region, they do not decipher the snowmelt processes that create water available for runoff (WAR). Nevertheless, those studies that have focused on melt processes have suggested that "energy budgets of snowmelt during rain-on-snow

events show that the relatively 'warm' rain provides little energy to melt snow. Rather, the primary source of energy to melt snow is the condensation of water vapor onto the snow pack" (Wondzell and King, 2003, pg. 82). In their definitive study at the WBSL, the U.S. Army Corp of Engineers stated that "no measures of solar radiation were obtained at WBSL because of its expected minor importance in the direct melt process at this location" (U.S.A.C.E., 1956, pg. 209). In addition, for the PNW there is also a general notion that ground heat flux is not an influential component to the EB (Berris and Harr, 1987), that open sites produce more melt and water available for runoff than forested sites (Marks et al., 1998; Berris and Harr, 1987), and that shallow snowpacks are most important for ROS where snowpacks melt out completely over the course of the single ROS event which have greater influence on runoff (Marks et al., Berris and Harr, 1987). To date, we have not had the datasets to test these generalizations. What we do know is that big floods in the PNW are often caused by ROS, but that these large flood events are uncommon. The few experimental studies in this and other regions have shown that turbulent exchanges are a large portion of the EB during ROS events and a dominant driver of melt.

Recent modeling approaches (Garen and Marks, 2005; Hardy et. al. 2000; Link and Marks, 1999b) have used various techniques to account for snow surface albedo. We compared our approach to others (Garen and Marks, 2005; Link and Marks, 1999b) in order to evaluate the energy balance results. This will help to identify how improvements can be made to routines which account for debris on the snow surface.

To improve our understanding of the snowmelt regime in the PNW, we use a physically-based snow energy and mass balance model (SNOBAL, Marks et. al.,

1999b) to simulate snow accumulation and melt, and to inform questions on the relative importance of the various energy balance components at different temporal scales and topographic settings. We use the model and the impressive time series of snow accumulation and melt data from the HJA Long Term Ecological Research site to test the "conventional wisdom" about the snowmelt processes in PNW. We use SNOBAL as a learning tool to better understand processes which are difficult to measure and quantify, in order to provide additional perspective on single-event focused work (e.g. of Berris and Harr, 1987 and of Marks et al., 1998, who focused on the 1996 event). This is the first time that numerous ROS events of varied intensities has been evaluated to truly characterize the PNW snowmelt regime.

The main research questions of this paper are:

1. What are the EB components of snowmelt at HJA on an annual basis?
2. How does their relative importance change with different timescales?
3. What are the dominant components of the EB during high-frequency ROS events?
4. How much annual snowmelt comes from ROS events vs. non-ROS event melt?
5. How do energy balance components vary by site elevation, exposure, aspect?

2.2 METHODS

2.2.1 Snow Energy Balance

The snow energy balance describes the amount of energy contributing towards snow melt (Q_m). It is described as:

$$Q_m = R_n + L_n + H + L_{ve} + G + M \qquad \text{Equation 2.1}$$

where R_n is net shortwave radiation, L_n is net longwave radiation, H is sensible heat exchange, L_{ve} is latent heat of evaporation, G is the ground heat flux, and M is advected heat from precipitation. Net shortwave radiation (0.3 to 2.8µm) is the total amount of solar radiation absorbed by the snowpack. Net longwave radiation is the amount of energy incident on the snow from the atmosphere and surrounding vegetation, less the amount of emitted thermal radiation from the snowpack. Sensible and latent heat are the turbulent exchanges and are highly dependent on wind speed. Sensible heat is the amount of convective heat transfer at the snow-air interface. Latent energy flux is a result of evaporation, condensation, or sublimation. Ground temperatures are often measured to be above or near 0°C, therefore it is necessary to account for the energy conducted from the soil-snow interface. Differences in temperature between precipitation and the snowpack, results in advected heat transfer. The energy available for melt is then added to the cold content, which is the amount of energy needed to bring the snowpack to isothermal conditions. If the energy available for melt is negative, then there is a net loss of energy from the snowpack.

2.2.2 Study Site

The study sites are located within the HJA Experimental Forest, a part of the Long-Term Ecological Research (LTER) program. The experimental forest is located in the western Oregon Cascade Range, and encompasses the 62 km^2 drainage of Lookout Creek, a tributary to the Blue River in the McKenzie River basin. Elevations in the HJA range from 800 to 2000 m. The Mediterranean climate produces approximately 80% of annual precipitation in the months between November and March, whereas summers are typically warm and dry (Figure 2.1). Annual

precipitation ranges from 1800 to 3000 mm in the upper elevations. Above 1000 m, winter precipitation falls mainly as snow. The transient snow zone lies roughly between 500 and 1000 m. At these elevations, snow and rain are frequent in the winter months, with ROS events common. However ROS events do occur at all elevations of the HJA during the winter. The elevation range and climate (Greenland, 1994) of the HJA are typical of the western Cascades in Oregon.

We used data from three permanent climate stations in the middle to upper elevations of the Lookout Creek basin: Central (1018 m) (CENMET), Vanilla Leaf (1273 m) (VANMET), and Upper Lookout (1294 m) (UPLMET) (Figure 2.2). Each site has a similar array of sensors: air temperature, relative humidity, precipitation, incoming solar radiation, wind speed, ground temperature, and snow water equivalent (SWE) (Table 2.1). These sites have nearly complete records for water years 1996 to 2003, providing a unique dataset to apply our physically based snow energy balance model.

Temperature and relative humidity were monitored using a Campbell Model HMP35C housed in a PVC radiation shield. Solar radiation was measured using a Kipp & Zonen model CM-6B pyranometer (spectral range: 0.3 to 2.8 μm). Wind speed was measured by a RM Young anemometer mounted at 10 m above ground. Soil temperature measured by Campbell Scientific thermistor probes at 20 cm was used for this investigation.

Cumulative precipitation gauges were located at each climate station. The VANMET precipitation gauge was a heated standing pipe with an alter wind shield. The CENMET precipitation gauge was located on the shelter house and utilizes the

shelter's propane heating system. The primary precipitation gauge at UPLMET was a stand-alone gage with a Valdais wind shield. Butyl snow pillows were located at each of the stations to measure SWE. Manual snow depth and SWE measurements were also taken periodically by field personnel.

2.2.3 ROS Definition

Harr (1983) defined ROS as *rain falling on a snowpack*. This simple definition does not account for negligible precipitation amounts that often fall upon the snowpack which does not produce melt or water available for runoff. In this paper, we define ROS events at the HJA to be *8 consecutive 3-hour time steps (24 hours) during which rainfall is reported (0.254mm) to fall on a snow covered surface*. Using this definition allows us to evaluate a number of small ROS events and their contribution to melt and WAR, whereas previous studies have focused on larger events. Adjusting the required time period (Table 2.2) for consecutive rainfall occurrences did not significantly affect the number or range of ROS events for this analysis.

2.2.4 SNOBAL

SNOBAL is a physically-based snow energy and mass balance model, developed (Marks, 1992) and described in detail by Marks et. al. (1999b) (Figure 2.3). The model has been applied at a number of locations including central Canada (Link and Marks, 1999a), Turkey (Sensoy et. al., 2006), and the Pacific Northwest (Marks et. al., 1998; van Heesjwick et. al., 1996). The spatially distributed version (ISNOBAL) has been successfully applied to the Boise River Basin (Garen and

Marks, 2005), the Wasatch Range in Utah (Susong, 1998), BOREAS (Link and Marks, 1999b), the California Sierra Nevada (Marks et. al., 1999a), the Reynolds Creek Experimental Watershed (Marks and Winstral, 2001; Winstral and Marks, 2002), and the central Washington Cascades (Mazurkiewicz et. al., *in prep.*). SNOBAL is a utility built in the Image Processing Workbench (IPW) (Frew, 1990; Marks et. al., 1999b). The software operates in a UNIX environment with a command line interface. In addition to SNOBAL, IPW utilities were used to calculate thermal radiation, relative humidity to vapor pressure conversions, and clear sky solar radiation (Marks et. al., 1999b).

2.2.5 SNOBAL Forcing Data

The required forcing data for the model are net solar radiation, incoming thermal radiation, air temperature, precipitation, wind speed, vapor pressure, and ground temperature. These forcing data were processed at 3-hour intervals for model runs.

2.2.5.1 Solar: The model requires net incoming shortwave radiation data (0.3 to 2.8 µm), which were generated from each station's measured incoming solar radiation. In order to account for reflected shortwave radiation, a modeling approach was taken because direct measurements of albedo were not available at the study sites. The measured incoming solar radiation data is integrated over the spectral range of 0.3 to 2.8 µm. However, snow surface albedo varies by wavelength. The radiation data were split into two bands (visible: 0.3 to 0.7 µm and near-infrared-NIR: 0.7 to 2.8 µm) in order to apply a different albedo value to each wavelength band. The IPW utility *twostream* (Meador and Weaver, 1980) was used to estimate the fractions of incoming

solar radiation, for clear sky conditions, in the visible wavelengths (48%) and in the NIR wavelengths (52%). These fractions were applied to the measured data to determine incoming shortwave radiation in each wavelength band. A clean-snow-surface albedo model in IPW, *albedo*, was used to calculate snow surface reflectance in the visible and NIR wavelengths based on surface grain size growth. These albedo values were then applied to the calculated wavelength bands.

Surface deposits of debris, such as branches, needle fall, and dust decrease the effective albedo of the snow surface (Hardy et. al., 2000). This process plays an important role in the radiation balance of PNW snowpacks. The climate of the PNW creates snowpacks that are at or near isothermal conditions throughout the winter resulting in snowmelt through the winter months. As snow depth decreases, more debris concentrates at the surface, reducing the snow albedo. In order to account for changes in surface debris, an albedo reduction algorithm was applied:

$$a_r = 0.0607 * \ln(TimeSincelastSnowfall) + 0.01398 \qquad \text{Equation 2.2}$$

This algorithm reduced the snow albedo over a 14-day period to a lower limit of 0.6 for visible and 0.4 for NIR wavelengths, an approach similar to that of Garen and Marks (2005). The coefficients in Equation 2.2 were developed by calculating a logarithmic decay for snow albedo from unity to 0.6 for the visible spectral range.

2.2.5.2 Thermal: Thermal (longwave) radiation was the only forcing parameter not measured directly. Longwave radiation input was estimated using a three-step process (Garen and Marks, 2005; Susong et. al., 1999). First, clear sky thermal radiation was estimated following the Brutsaert method with the IPW command, *trad*. This technique used air temperature, vapor pressure, and elevation to

approximate downwelling atmospheric thermal radiation during clear sky conditions. An adjustment of thermal radiation was required in order to account for the increased incoming longwave radiation from low, dense clouds that are common during winters in the PNW. A cloud cover factor was calculated using the methodology described by Garen and Marks (2005). The IPW *twostream* (Meador and Weaver, 1980) model was used to calculate incoming shortwave radiation for afternoon clear sky measurements. The model parameters were calibrated to fit known sunny day conditions. The model was then run for the entire modeling period and compared to daily values at 1200 and 1500 Pacific Standard Time. A ratio of the modeled and measured incoming solar radiation for these time steps was then calculated to give a daily cloud coverage fraction. This ratio was incorporated into a linear regression model developed by Garen and Marks (2005), which is based on measured thermal radiation.

The sites at the HJA are located in clearings characterized as forest openings, and are subject to emitted thermal radiation from vegetation. To account for vegetation thermal radiation (L_v) an algorithm for gray body emittance was used as suggested by Link and Marks (1999b):

$$L_v = (1-t)\varepsilon\sigma T^4 \qquad \text{Equation 2.3.}$$

where t is transmissivity, ε is emissivity, σ is the Stefan-Boltzmann constant, and T is vegetation temperature in Kelvin. This method applies the Stefan-Boltzmann equation accounting for emissivity and transmissivity of vegetation based on field results from Link and Marks (1999b). The temperature of the vegetation was assumed to be air temperature, transmissivity of thermal radiation was assumed to be 0.75, and emissivity to be 0.96. Calculated thermal radiation from vegetation was then added to

the calculated atmospheric thermal radiation. The result was the modeled downwelling thermal radiation for SNOBAL, accounting for location, cloud cover, vegetation, and atmospheric conditions.

2.2.5.3 Air temperature: Air temperature (°C) was measured at 450 cm above the soil surface at each site and averaged for 3-hour time steps. Where data at 450 cm were missing or questionable, data from sensors at 350 cm were adjusted using a simple linear regression transfer function. Transfer functions were calculated by creating linear regressions between the 450 cm and 350 cm air temperature sensors at each station. WY 1999 was omitted in this analysis at VANMET because of faulty air temperature data.

2.2.5.4 Wind speed: Wind speed measurements were made at each site at 10 m above the ground surface. Average wind speeds were calculated over three hour time periods and used in the model.

2.2.5.5 Vapor Pressure: Vapor pressure is the amount of pressure exerted by water vapor molecules in a given volume of air Relative humidity measurements were collected at each site and were used to calculate vapor pressure (Pa) and dew point (°C). The calculations were carried out in IPW utilities *rh2vp* and *dewpt*.

2.2.5.6 Precipitation: Precipitation data from each site were used. Short intervals, up to 2 weeks, of missing or questionable data may have resulted from snow plugs in the precipitation gauges, datalogger failure, or undercatch. In addition to short periods of inadequate data at each station, the water year (WY) 1997 record at VANMET was entirely missing. Missing values were estimated using transfer functions based on long, concurrent records at the three stations. The variability of

precipitation over three-hour time periods limited our ability to develop strong correlations for short-time periods. Precipitation totals for storm events were a more accurate representation of site correlation and were used to correlate precipitation between sites.

UPLMET was chosen to fit VANMET storm totals, due to their similar elevations (Figure 2.2) and known correlations of elevation and annual precipitation amounts. A transfer function for precipitation events was developed for the eight-year period. In order to have an estimate of the timing of the precipitation throughout each event, it was assumed that the fraction of the storm total for each time step which fell at UPLMET was the same at VANMET for the missing records. The assumption was then be evaluated in the SNOBAL results for water year 1997.

Precipitation temperature and type were estimated using dew point temperature calculated at each site. A threshold of 0.5°C was used to delineate between snow and rain at VANMET and UPLMET. The threshold was determined by using SNOBAL to test threshold temperatures which would most closely follow measured accumulation patterns. The 0.5°C dew point temperature threshold did not provide the proper accumulation amounts at CENMET compared to SWE measurements. Field experience has noted snow events at low elevation above 0.5°C. It was determined that a threshold of 1.0°C provided the proper amount of snowfall to create model accumulation patterns which fit measurements of SWE.

2.2.6 Energy Balance Analysis

To investigate the effects of time period analysis on the variability in the EB components, energy inputs were subdivided for WY 1996 to biweekly and event scale.

WY 1996 was chosen for further analysis because of a major ROS event which occurred in February. The large ROS event of early February 1996 has been documented at other bcations (Marks et. al., 1998). This event produced flooding along the western slope of the Cascades, caused by high precipitation and melting of low-elevation snowpack. The calculated values of EB components were compared to Marks et. al. (1998) to determine if modeled results for two different datasets in the same region were comparable for the same event.

2.3 RESULTS

SNOBAL produces modeled energy fluxes of net radiation, ground heat, sensible heat, latent heat, and advected energy. Snowpack conditions simulated include SWE, melt, snow depth, cold content, evaporation (positive and negative), and snowpack temperature. Measured and modeled SWE were used to calculate a Nash-Sutcliffe (NS) model efficiency coefficient (ME) at each site for the periods of available snow pillow data:

$$ME = 1 - \left[\frac{\sum_{i=1}^{n} \left(x_{obs} - x_{sim} \right)^2}{\sum_{i=1}^{n} \left(x_{obs} - \bar{x}_{obs} \right)^2} \right] \qquad \text{Equation 2.4}$$

where n is the number of observations, x_{obs} is the observed measurement, x_{sim} is the simulated, and $\bar{x}_{obs}$ is the average of the observed measurements. Snow pillow data was available for WY 1996 to 2000 at UPLMET; WY 1997 to 2003 for VANMET; and 1997 to 2003 at CENMET (Figure 2.4). Only the time steps for which modeled or measured snowpack existed were included in the NS calculations. The ME for UPLMET and VANMET were 0.94 and 0.93, respectively. The ME calculated for

CENMET was 0.76. Modeled SWE matched well with measured SWE data during accumulation and melt periods at all three sites. The model did have difficulties producing early season snow accumulation patterns that matched measurements. This is due to the high measured ground temperatures, which resulted in fast melting snow. Snow pillows have been shown to greatly influence ground heat flux (Johnson and Schaefer, 2002). This may result in some discrepancies because bare ground conditions are simulated by SNOBAL. The model has the most difficulty matching conditions at CENMET in snow years where the snowpack accumulated and melted multiple times. The SNOBAL SWE prediction at VANMET for WY 1999 is lower than measured SWE accumulation. This is because of faulty air temperature readings at the station during that water year, which is excluded from the analysis.

2.3.1 Energy Balance

Energy balance components at the three hour model time step were analyzed for water years 1996 to 2003. Net radiation was the dominant driver of snowmelt at the HJA (Figure 2.5). The turbulent fluxes of latent and sensible heat melted considerably less snow than radiation at all sites. Turbulent fluxes were most important at VANMET (24% of melt). Ground heat flux contributed a surprisingly large amount of energy to the snowpack at VANMET (18%) and especially CENMET (29%). Advected energy from rain was relatively minor at all sites (<3%).

At the annual scale, the relative contribution of net radiation flux to snowmelt was uniformly high at UPLMET, ranging from 71 to 87%, and averaging 80% (Figure 2.6). Radiation at CENMET and VANMET was also the most important driver of melt, but to a lesser degree and with higher year-to-year variability. The importance

of the combined turbulent fluxes (latent and sensible heat) varied annually by site. At UPLMET, the contribution of turbulent fluxes to the snowpack was relatively small, with little inter-annual variability (9 to 12%). Turbulent fluxes at CENMET and VANMET had greater variability from year to year. Ground heat flux, particularly at the lower-elevation site (CENMET: 15 to 55%), was the most variable contributor to snowmelt from year to year. Advective heat transfer was uniformly low at all sites.

The UPLMET energy balance was examined at biweekly and event scales for water year 1996. The biweekly analysis showed a seasonally varying pattern of the relative importance of the energy balance components (Figure 2.7). Early-season snowmelt was driven predominantly by ground heat flux, whereas snowmelt after the peak snowpack date was generally driven by radiation.

2.3.2 ROS events

The UPLMET energy balance was examined for a major ROS event (February 1996) of 168 hours at three-hour intervals (Figure 2.8). Turbulent energy fluxes were important during this event, although net radiation also positively contributed to energy for snowmelt. Measured rainfall for the event was 286 mm at UPLMET, which was reflected in the high advected energy flux. As at longer time scales, the event-scale energy balance component contributions to melt varied by site for this event (Table 2.3); turbulent energy exchange was most important at VANMET. February 9-10 in Figure 2.8 shows the typical dry-weather pattern of radiation flux alternating between night (net radiation loss from the snowpack) and day (net radiation gain).

Using our definition of a ROS event, model output at each site was separated into ROS and non-ROS periods. The number of events, precipitation amounts, and melt amounts for all of these events varied by site (Table 2.4). The highest average ROS melt rate was observed at VANMET. However, average melt rates for ROS events did not differ substantially from non-ROS melt rates. Average energy fluxes over the ROS record for each site were calculated (Figure 2.9). Net radiation flux was the dominant contributor to snowmelt during ROS events. The combination of the turbulent energy fluxes were the most important driver of melt during ROS events at VANMET, accounting for 42% of snowmelt. At CENMET, net radiation and turbulent exchanges were similar for ROS events. Ground heat flux contribution to melt during ROS events ranged from 8 (UPLMET) to 24% (CENMET). Advective transfer to the snowpack was relatively high during ROS events, at 10 (VANMET) to 15% (UPLMET).

The percentage of snowmelt generated during ROS events on an annual basis over the eight-year record ranged from 3-20% and averaged 8 to 12% at the three sites. Although total WAR produced during ROS events was often a large percentage (6 to 42%) of the annual total, WAR which occurred during ROS events was primarily composed of precipitation which percolated through the snowpack (Figure 2.10). Percolating precipitation was identified as the amount of WAR less the amount of rainfall which fell on the snowpack. CENMET had the highest contribution of precipitation to WAR (annual average of 28%), although values at the two higher-elevation sites were similar. ROS events contributed the most to annual WAR at CENMET (62% for 1996), but average annual ROS (rain plus snowmelt) contribution

to WAR ranged from 30% (UPLMET) to 39% (CENMET). Except for two years at CENMET, the majority of annual WAR was snowmelt produced by non-ROS processes.

2.4 DISCUSSION

The dataset that has been presented allows us to analyze and interpret multiple years of snow energy balance. Past work, which has focused on the event and seasonal temporal scales, has helped to interpret dominant process in short windows of analysis. Using the HJA climate dataset and SNOBAL as an investigative tool to separate EB components, melt water, WAR, and rainfall percolation through the snowpack, can help us to understand the processes that are most influential in creating melt and WAR inputs to streamflow.

Modeled SWE matched well with measured SWE at all three sites, although the fit varied between sites. Modeled SWE generally matched measured SWE more closely during years with deeper snow. Seasons with shallow snowpacks, or in the case of CENMET, transient snow years, were more difficult for the model to simulate. SNOBAL has been developed and tested in seasonal snowpack climates but has not been used extensively in the transient snow zone.

2.4.1 Energy balance variability

For water years 1996 to 2003 we found that the net radiation balance was a dominant contributor to the energy for melt at each of the sites: UPLMET, 80%; VANMET, 55%; CENMET 49% (Figure 2.5). These contributions are surprisingly high for an environment that has been classified as a rain-on-snow dominated

(U.S.A.C.E., 1956). Previous work by Berris and Harr (1987) and Marks et. al. (1998) has shown how important turbulent fluxes are during rain-on-snow events in the PNW forested environments. These fluxes were assumed to be the dominant processes in the HJA which straddles the transient snow zone and experiences numerous rain-on-snow events throughout the winter season.

The variability of net radiation contributions to melt reflected the timing of melt out at each station. Snow which existed later into the spring was subject to the longer daylight hours and more intense incoming radiation in late spring. Conversely, shallow snowpacks melted out earlier in the season and were therefore exposed to fewer high net-radiation-flux days. During springtime, nighttime temperatures typically remain above freezing which supports an isothermal snowpack. The isothermal snowpack is then subject to high radiation input, which produced high melt rates. This resulted in high positive radiation fluxes which caused a majority of the annual snowmelt regime.

Over the eight-year record, snow melted out sooner at VANMET than at UPLMET. The UPLMET and VANMET sites are at a similar elevation, but nearly opposite aspects. VANMET faces south, and is therefore exposed to the prevailing winds during winter and spring storms, whereas UPLMET's north aspect provides shelter from prevailing winds and incident solar radiation. Accordingly, turbulent energy fluxes were higher at VANMET than at UPLMET. Although VANMET is more exposed to direct-beam solar radiation than UPLMET, radiation was a more important driver of annual snowmelt at UPLMET. This is due to the late season snowpack at UPLMET which is subject to high solar insolation during the late spring.

The CENMET site is 300 meters lower in elevation than UPLMET and VANMET, with a southeast aspect. Annual snow accumulation is much lower than the two other study sites. The elevation and air temperature at CENMET appears to play a key role in controlling the snow regime. Elevation temperature lapse rate results in warmer temperatures and higher dew point temperatures. This reduces the amount of annual snow accumulation on the ground and reduces the number of snow events at the site. The warmer air temperatures at the site drive turbulent energy fluxes reducing the amount of winter snow accumulation. Shallow snow accumulations in early winter are subject to warm ground temperatures, causing fast melt out, which is reflected in high ground heat flux during low snow years.

If we quantify EB components for the accumulation and melt season separately, a different picture emerges. During early to mid-winter, relatively little snow melts, especially at the upper sites. Melt that does occur during this period was driven mainly by ground heat flux. Ground temperatures were typically above 0°C, with temperatures well above freezing throughout the fall and prior to snowfall. Consequently, shallow, early-season snow tended to melt quickly. These results would be sensitive to soil thermal conductivity within the model. As the snowpack accumulated, ground temperature remained steady at temperatures just above freezing. The snowpack generally showed a loss of net radiation due to shorter days and generally cloudy weather. This limited incoming shortwave energy, while high snow surface albedo reflected a large proportion of the radiation which did reach the snowpack. Turbulent fluxes were positive throughout the winter period, but low due to low temperature and vapor pressure gradients and generally low wind speeds.

2.4.2 ROS

2.4.2.1 1996 Event

During the February 1996 ROS event, melt rates and energy balance components were influenced by high wind speeds with warm, moist air. This created conditions for high turbulent energy fluxes and added moisture the snowpack through condensation. Model calculations also showed a net gain of radiation throughout the event. Net shortwave radiation inputs were low due to clouds, while the warm temperatures and high humidity increased the incoming thermal radiation from the low cloud cover. Turbulent fluxes were not calculated to be as high as Marks et. al. (1998), because of lower wind speeds measured at UPLMET compared to locations used by Marks et. al. (1998) elsewhere the Cascades. Our calculated advected heat fluxes were also seen to be higher than Marks et. al.(1998). The technique to estimate precipitation temperature using dew point temperature was the same in our study and in Marks et. al. (1998). Resulting higher advected fluxes in our study may be due to higher local temperature caused by topographic position of VANMET, CENMET, and UPLMET in the HJA. Local topographic features may allow warmer low elevation air to be pushed up the basin and trapped causing warmer local temperatures and higher dew point temperatures.

2.4.2.2 High Frequency ROS

One focus of snowmelt-process research in the Pacific Northwest has been ROS events (Harr, 1981; Berris and Harr, 1987; Marks et al., 1998). These studies have shown that peak-flow events in the transient and transitional snow zone are often characterized by shallow snow at low elevations and high rainfall amounts coupled

with high wind speeds. WAR is produced by two main processes: melt from within the snowpack and percolation of rainfall through the snowpack. Shallow snowpacks and preferential flowpaths allow for shorter travel time of the rainfall through the pack and into the soil. In addition to the percolation of rainfall, water is added to the snowpack through condensation. Condensation adds water and releases energy into the snowpack, contributing to the net energy available to melt snow. This process requires high turbulent exchanges rates controlled by wind speeds. Marks et. al. (1998) showed that forested areas have much lower turbulent exchanges due to lower wind speeds.

Field and modeling approaches have extended our knowledge of the melt processes which dominant ROS events. Large events, such as the February 1996 event, result in regional flooding due to high amounts of rain on a low elevation snowpack, warm temperatures, and high wind speeds. Events this extreme are not common in this PNW. In the eight-year HJA dataset, we identified 83 ROS events at an upper elevation site (UPLMET) and 56 events at a lower elevation site (CENMET). The longer-duration snowpack at the higher elevation site was exposed to more rain events over the course of the snow seasons. The highest event rainfall amount at each site was the February 1996 event (Table 2.4).

Our analysis of ROS events for the entire model period showed radiation dominated the EB during ROS melt at UPLMET (Figure 2.9). This site is protected from the dominant wind direction during storm events resulting in lower turbulent exchange rates. The deeper snowpack that often exists requires large amounts of energy to initiate melt. In contrast VANMET during ROS events is dominated by the

turbulent exchanges. This is also reflected in the annual energy balance and caused by higher measured wind speeds. CENMET's approximate equal contribution of turbulent and radiation energy inputs is a reflection of the timing of ROS events in the year. Due to the shorter snow season at CENMET the ROS events do not occur during periods with high incoming solar insolation reducing the amount of overall net radiation inputs. Warmer air temperatures which occur during ROS events is shown in the relatively high amount of turbulent exchange inducing melt during ROS events.

High frequency ROS events contributed a small amount of melt over a winter season (Figure 2.10). Lower-intensity events (in contrast to the February 1996 event) have lower wind speeds and result in lower turbulent exchanges. During average ROS events, net radiation was a positive contributor to the energy balance and to snowmelt. Cloud cover reduced the net solar radiation balance even though radiation contributions to the energy balance were positive.

Rain-on-snow events accounted for about 35% of WAR during the snow season, leaving a surprisingly high amount of annual WAR produced by non-ROS melt events. Spring melt driven by radiation produced the highest amount of WAR at all three locations. However, our results show that a majority of WAR produced during ROS events was precipitation and not snowmelt (Figure 2.10). Energy inputs into the snowpack during ROS events are relatively low. This is because of reduced incoming solar radiation, which has been shown to be the largest contributor to melt. Without a high net radiation input high melt rates can only be reached with high turbulent exchanges driven by turbulent fluxes as shown by Berris and Harr (1987).

Melt rates during ROS events are site specific. VANMET showed high average melt rates, coinciding with higher speeds, generating high turbulent energy exchanges. This process coupled with shallow snowpacks generated a high flux of precipitation through the snowpack resulting in high WAR during ROS events.

2.4.3 Evaluating Net Solar Radiation Modeling

Net solar radiation (0.3 to 2.8µm) inputs to the snowpack are controlled by atmospheric conditions, solar angle, duration of daylight hours, and albedo. Incoming solar radiation to the atmosphere and the effects of solar angle and topography are generally well understood, while our understanding of snow surface albedo in forested catchments for modeling applications is still limited. Clean snow albedo has been well correlated with snow surface and grain size (Wiscombe and Warren, 1980). Although the process of grain size growth can be estimated over time (Marks et. al., 1999b), the effects of vegetation and atmospheric deposition of debris on the snow surface is poorly understood. Recent modeling approaches (Garen and Marks, 2005; Link and Marks, 1999b) account for the increased snow surface debris by applying simple decay functions from peak snowpack to melt out. Although these approaches result in good model fit of measured SWE, measurements of SWE are required at the site. This technique is unsuitable for modeling areas with no or limited measurements, as is often the case with SWE. In contrast to other approaches, our model relies on a continuous deposition of litter and atmospheric debris on the snow surface, which is common in forested regions, and not on timing of peak snow pack to melt out. This technique is effective for the PNW forested snow zone, because of the near-isothermal

snow pack. This results in small melt events throughout the snow season, allowing debris to accumulate at the snow surface, reducing the snow surface albedo.

We evaluate our approach in comparison to other published albedo decay models, to identify discrepancies in model performance and see the effects of different albedo modeling decay approaches on the annual snow energy budget summary. Garen and Marks (2005) applied a square root decay function with lower limits for the visible and NIR, modeled from peak snow pack to melt out. Link and Marks (1999b) used a linear decay function from peak snow pack to melt out. We applied these two approaches to the UPLMET WY1996 dataset (Figure 2.11). Neither albedo decay model produced SWE estimates that track the snow pillow data. Nash-Sutcliffe coefficients for the linear and square-root albedo reduction models are 0.87 and 0.86, while the dynamic model ME was 0.97. This implies that there is a deficit of incoming radiation to the snowpack to create the melt that is measured at the site. The dynamic albedo model that we applied tracks the measured SWE, following the melt rates closely.

These three albedo decay models all produce similar results in an annual snow energy balance budget (Figure 2.11), with radiation being the largest contributor to melt at UPLMET for WY 1996. This annual energy budget indicates the influence of solar radiation in creating melt through the spring melt.

2.4.4 Evaluating Ground Heat Flux

Ground heat flux is often thought of as negligible in snow energy budgets (Male and Gray, 1981). This has led to many distributed modeling approaches that assume a ground temperature of 0°C. Our energy balance results contradict this

assumption. Positive ground temperatures are often measured beneath a snowpack, which causes small amounts of melt throughout the winter, contributing to snowpack metamorphism. These mid-winter contributions were minor in our evaluation of UPLMET data at a bi-weekly time step (Figure 2.7). However, early-season snowfall on a relatively warm, bare ground surface results in rapid melt. The integrated contribution of this energy over the annual energy budgets is surprisingly large. Measured soil temperatures at multiple depths (Figure 2.12) showed soil temperatures throughout the snow season were above 0°C. Fluctuations in temperature reflected melt water pulses through the soil profile. The uncertainty of this energy contribution lies within the calculation of effective heat transfer from the soil to the snow. This calculation within the model (Marks et al., 1998) relies on thermal conductivity measurements of bare mineral soils, which may not portray the conditions that exist in the HJA.

2.4.5 Implications

The point-scale modeling approach has allowed us to identify clear differences in snowmelt regimes within a mesoscale watershed. These differences are important for distributed snowmelt modeling. The substantial differences in energy balance, snow accumulation and melt regimes at two sites in close proximity and at the same elevation (UPLMET and VANMET) cast doubt on the validity of traditional approaches to distributing snowmelt. Modeling approaches that use lapse rates to distribute precipitation, temperature and wind speed would treat these two stations identically for these parameters.

It is necessary to carefully consider the topographical and vegetation interactions with boundary layer conditions. This is especially apparent in our analysis of EB components during ROS events. VANMET has higher turbulent exchanges during these events, caused by higher measured wind speeds, the result of its topographic position on a south facing slope. This aspect is subject to frontal winds increasing the overall turbulent exchanges. High melt values were also measured here during these events, which may be due to its southern aspect as well. This makes the site subject to high incident solar radiation throughout the winter, contributing to lower cold contents. UPLMET is a protected site from the southern frontal winds. The site accumulates more snowpack resulting in less melt during ROS events. Berris and Harr (1987) also found that deeper snowpacks contribute less to WAR, because of the higher cold content and water holding capacity.

2.4.6 Limitations and Future Work

The extended, high-quality dataset allowed us to perform a thorough analysis of energy balance components. However, albedo data were not available which is critical in correctly estimating the contribution of incoming shortwave radiation. The evolution of the albedo of clean snow is well-documented, but albedo variability in forested catchments ("dirty" snow) is considerable. Debris that is deposited randomly on the snow surface is difficult to measure and monitor. Hardy et. al. (2000) presented an algorithm to estimate the evolution of surface deposition, burial, and subsequent re-exposure. This routine requires a snow model which parameterizes snow surface albedo based on calculated snow accumulation and melt. Models such as this will become more useful, once there are more estimates of surface deposition rates in

different environments. There are no studies in the PNW which identify litter deposition processes in relation to snow hydrology. Studies like this in multiple forest types will help to better define albedo evolution for distributed modeling.

Thermal radiation from vegetation is not typically measured as a component of meteorological of climate stations. In order to estimate thermal emittance, air temperature is often used as a proxy for vegetation temperature. Hardy et. al. (2004) showed that this is not an accurate estimate of vegetation emittance. Vegetation temperatures are often much higher than the air temperature. Additional field measurements can help to create routines to more accurately estimate these inputs for physically-based models.

In our analysis of ROS events, percolating rainfall was determined to be the major contributor to WAR. Research has shown that flowpaths of water through snowpack exhibit preferential behavior (Male and Gray, 1981). The mixing of precipitation water with melt water, pathway length, and timing are poorly understood. Increased understanding of these processes will help us to create models that closely follow the water holding capacity and subsequent release of water to runoff.

2.5 CONCLUSIONS

This investigation into the controls of the snowmelt energy balance provides new incite into the dominant melt processes in the HJA. We found that net radiation dominated the snowmelt energy balance over the period 1996-2003 at our 3 measurements sites: UPLMET 80%, VANMET 55%, and at CENMET 49%. Annual variability in the EB components reflected the time duration of the snowpack (snow covered period). A snowpack which lingered into the spring resulted in higher

radiation as a percent of total EB components, while transient snow seasons resulted in higher percentages of turbulent exchange contributing the EB. Ground heat flux integrated over the modeling period proved to be a large contributor to the EB.

The relative importance of EB components for causing melt changed with different timescales. Annual melt regimes were dominated by the net radiation inputs. Bi-weekly timescales showed EB components varying with seasons. Low radiation inputs during winter months to high spring radiation inputs creating the most melt. At the event scale (1996 Storm) radiation was still a substantial contributor to melt. However turbulent energy fluxes comprised a large percentage (32%) of the EB during this major ROS event.

Radiation was the largest contributor to melt during ROS (UPLMET 55%, VANMET 35%, and CENMET 33%). These radiation inputs during ROS events have been overlooked often with the notion that high wind speeds coincide with ROS events. The EB components during ROS events varied by site. Elevation, exposure, and aspect to prevailing winds increase turbulent exchange.

Melt from ROS events is a small percentage of annual melt. For the period 1996-2003 snow season 80-90% of snowmelt comes from non-rain melt days. Over 75% of WAR during ROS is rainfall that percolates vertically through the snowpack.

2.6 ACKNOWLEDGEMENTS

We would like to extend our thanks and appreciation to David Garen and Danny Marks, who both have helped us along the way with running SNOBAL and offered critical feedback of model results. Critical manuscript reviews from Rick Woodsmith

and Anne Nolin were much appreciated. We also are grateful for the availability of data through the HJA LTER webpage.

2.7 REFERENCES

Berris, S., Harr, R.D., 1987. Comparative snow accumulation and melt during rainfall in forested and clear-cut plots in the western Cascades of Oregon. Water Resources Research 23, 135-142.

Hardy, J., Melloh, R., Robinson, P., Jordan, R., 2000. Incorporating effects of forest litter in a snow process model. Hydrological Processes 14, 3227-3237.

Hardy, J.P., Marks, D., Link, T., Koenig, G., 2004. Variability of the below canopy thermal structure over snow. *Eos Trans. AGU,* Fall Meet. Suppl., 2004.

Harr, R.D., 1981. Some characteristics and consequences of snowmelt during rainfall in Western Oregon. Journal of Hydrology 53. 277-304.

Harr, R.D., Berris, S.N., 1983. Snow accumulation and subsequent melt during rainfall in forested and clearcut plots in Western Oregon. Proceeding of the Western Snow Conference, 38-44.

Johnson, J.B., Schaefer, G.L., 2002. The influence of thermal, hydrologic, and snow deformation mechanisms on snow water equivalent pressure sensor accuracy. Hydrological Processes 16, 3529-3542.

Jones, J.A., Swanson, F.J. 2001. Hydrologic inferences from comparisons among small basin experiments. Hydrological Processes 15, 2363-2366.

Jones, J. A.., Grant G.E., 1996. Peak flow responses to clear-cutting and roads in small and large basins, western Cascades, Oregon, Water Resources Research 32, 959-974.

Garen, D. Marks, D., 2005. Spatially distributed energy balance snowmelt modeling in a mountainous river basin: Estimation of meteorological inputs and verification of model results. Journal of Hydrology 315, 126-153.

Greenland, David. 1994. The Pacific Northwest regional context of the climate of the H.J. Andrews Experimental Forest. Northwest Science. 69(2), 81-96.

Link, T., Marks, D., 1999a. Distributed simulation of snowcover mass- and energy-balance in the Boreal forest. Hydrological Processes 13, 2439-2452.

Link, T., Marks, D., 1999b. Point simulation of seasonal snowcover dynamics beneath Boreal forest canopies. Journal of Geophysical Research, Atmospheres 104(D22), 27841-27858.

Male, D.H., Gray, D.M., 1981. Snowcover ablation and runoff. In: Gray, D.H., Male, D.M. (Eds.), Handbook of Snow, Permagon Press, Willowdale, Canada, pp 360-430.

Marks, D., Kimball, J., Tingey, D., Link, T., 1998. The sensitivity of snowmelt processes to climate conditions and forest cover during rain-on-snow: A case study of the 1996 Pacific Northwest flood. Hydrological Processes 12, 1569-1587.

Marks, D., Link, T., Winstral, A., Garen, D., 2001. Simulating snowmelt processes during rain-on-snow over a semi-arid mountain basin. Annals of Glaciology 32, 195-202.

Marks, D., Domingo, Susong, Link, Garen 1999a. A spatially distributed energy balance snowmelt model for application in mountainous basins. Hydrological Processes 13, 1935-1959.

Marks, D., Domingo, J., Frew, J., 1999b. Software tools for hydro-climatic modeling and analysis, Image Processing Workbench (IPW), ARS-USGS Version 2. ARS Technical Bulletin 99-1, Northwest Watershed Research Center, Agricultural Research Service, Boise, Idaho, USA. Electronic document available on the Internet at http://cirque.nwrc.ars.usda.gov/~ipw.

Marks, D., Dozier, J., 1992. Climate and energy exchanges at the snow surface in the alpine region of the Sierra Nevada: 2. Snow cover energy balance. Water Resources Research 28, 3043-3054.

Marks, D., Dozier, J., 1979. A clear-sky longwave radiation model for remote alpine areas. Archiv für Meteorologie, Geophysik und Bioklimatologie, Serie B 27, 159-187.

Susong, D., Marks, D., Garen, D., 1999. Methods for developing time-series climate surfaces to drive topographically distributed energy- and water-balance models. Hydrological Processes 13, 2003-2021.

Serreze, M.C., Clark, M.P., Armstrong, R.L., McGinnis, D.A., Pulwarty, R.S., 1999. Characteristics of the western United States snowpack from snowpack telemetry (SNOTEL) data. Water Resources Research 35(7), 2145-2160.

Sensoy, A., Sorman, A. A., Tekeli, A. E., Sorman, A. Ü., Garen, D. C., 2006. Point-scale energy and mass balance snowpack simulations in the upper Karasu basin, Turkey. Hydrological Processes 20, 899-922.

U.S.A.C.E. (U.S. Army Corps of Engineers), 1956. Snow Hydrology. U.S. Army Corps pf Engineers, Portland, Oregon, 437 pp.

Winstral, A., Marks, D., 2002. Simulating wind fields and snow redistribution using terrain-based parameters to model snow accumulation and melt over a semi-arid mountain catchment. Hydrological Processes 16, 3585-3603.

Wiscombe, W. J., Warren, S. G., 1980. A model for the spectral albedo of snow I. Pure snow. Journal of the Atmospheric Sciences 37(12), 2712-2733.

Wondzell, S.M., King, J.G., 2003. Postfire erosional proceses in the Pacific Northwest and Rocky Mountain regions. Forest Ecology and Management 178: 75-87.

van Heesjwick, M., Kimball, J., Marks, D. 1996. Simulation of water available for runoff in clearcut forest openings during rain-on-snow events in the western Cascade Range of Oregon and Washington. Water Resources Investigations Report 95-4219 Geological Survey, Tacoma, Washington, 67 pg.

Table 2.1 Meteorological measurements

Parameter	*Sensor*	*Sampling Interval*	*Precision*	*Instrument Height (above soil surface)*
Wind speed	RM Young 05103 Sensor	15 min.	0.25 m/s	10 m
Air Temperature	Campbell Model HMP35C	15 min.	0.1°C	450 cm
Relative Humidity	Campbell Model HMP35C	15 min.	0.1	450 cm
Shortwave Radiation	Kipp & Zonen CM-6B	15 min.	0.05 langley	450-800 cm
Soil Temperature	Campbell 107	15 min.	0.1°C	20 cm depth
Precip	Stand alone gauge	15 min.	0.254 mm	

Table 2.2 Number of ROS events

	Number of ROS events for 3-hr timestep thresholds				
# of Timesteps	8	7	6	5	4
UPLMET	83	99	137	171	230
VANMET	61	77	100	125	161
CENMET	56	64	94	116	149

Table 2.3 EB components for 96 ROS event

site	*%Radiation*	*%Turbulent*	*%Ground*	*%Advected*
UPLMET	32	38	22	7
VANMET	21	54	8	16
CENMET	29	25	23	21

Table 2.4 ROS events at each station

Site	Number of ROS Events	Range of PPT (mm)	Average PPT (mm)
UPLMET	83	2.4 to 285.6	52.1
VANMET	61	8.5 to 301.99	52.33453
CENMET	56	4.8 to 321.07	62.48514

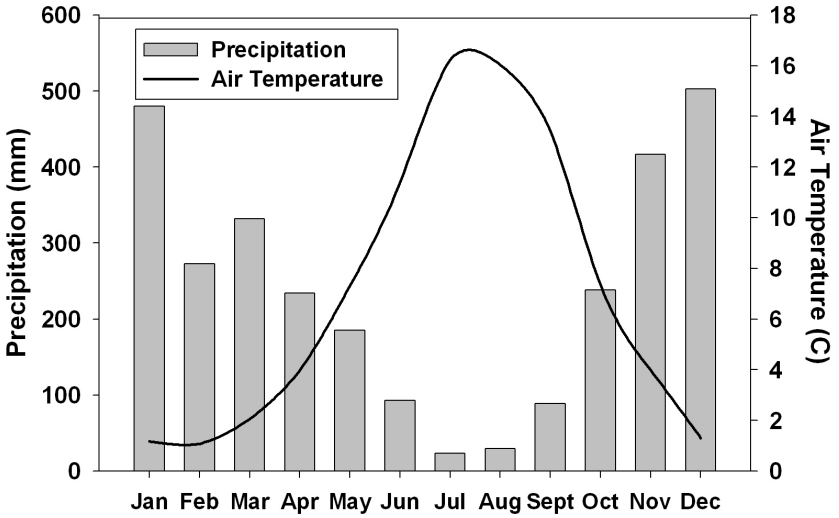

Figure 2.1 Climograph at Upper Lookout Meteorological station for years 1996 to 2003.

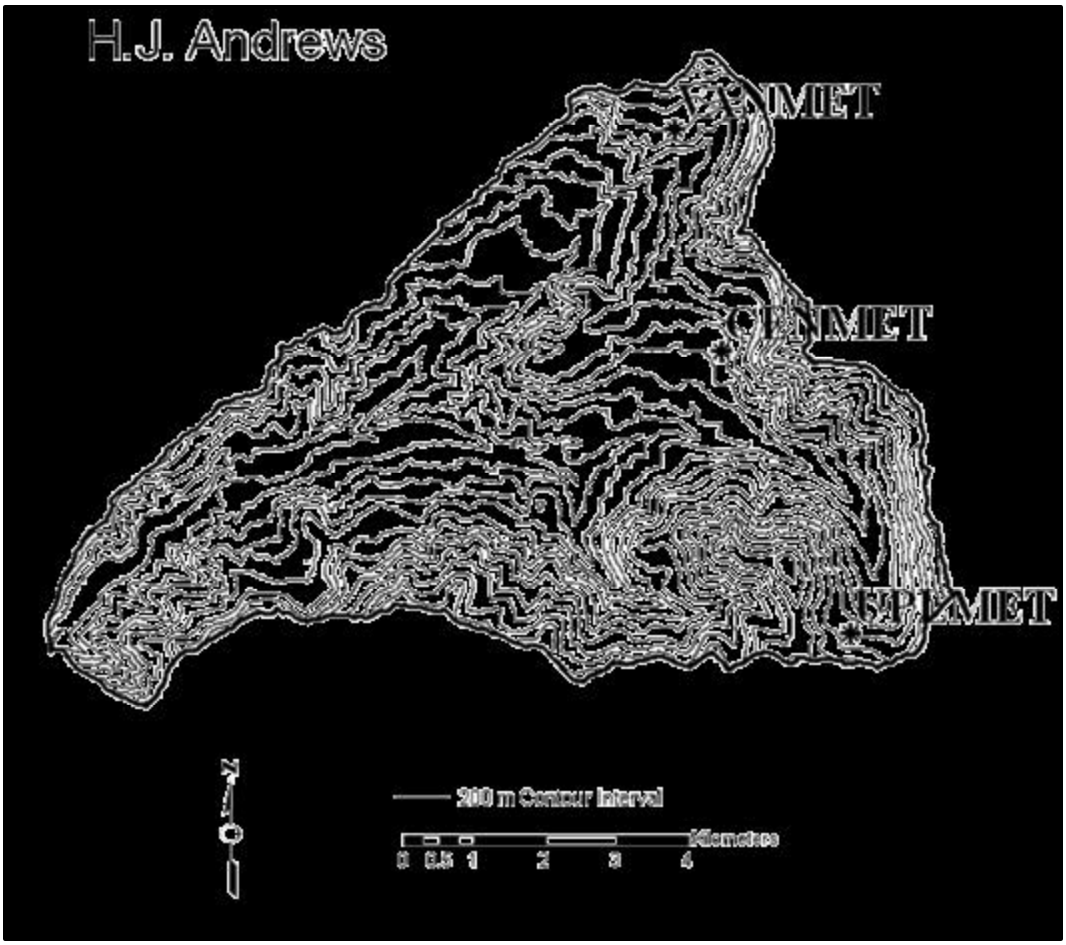

Figure 2.2 The H.J. Andrews Experimental Forest watershed, Western Oregon USA

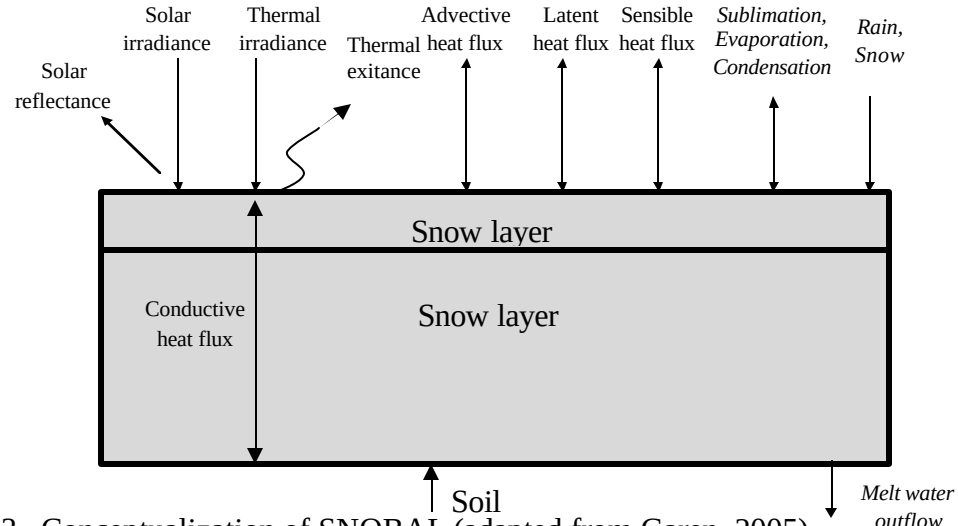

Figure 2.3 Conceptualization of SNOBAL (adapted from Garen, 2005).

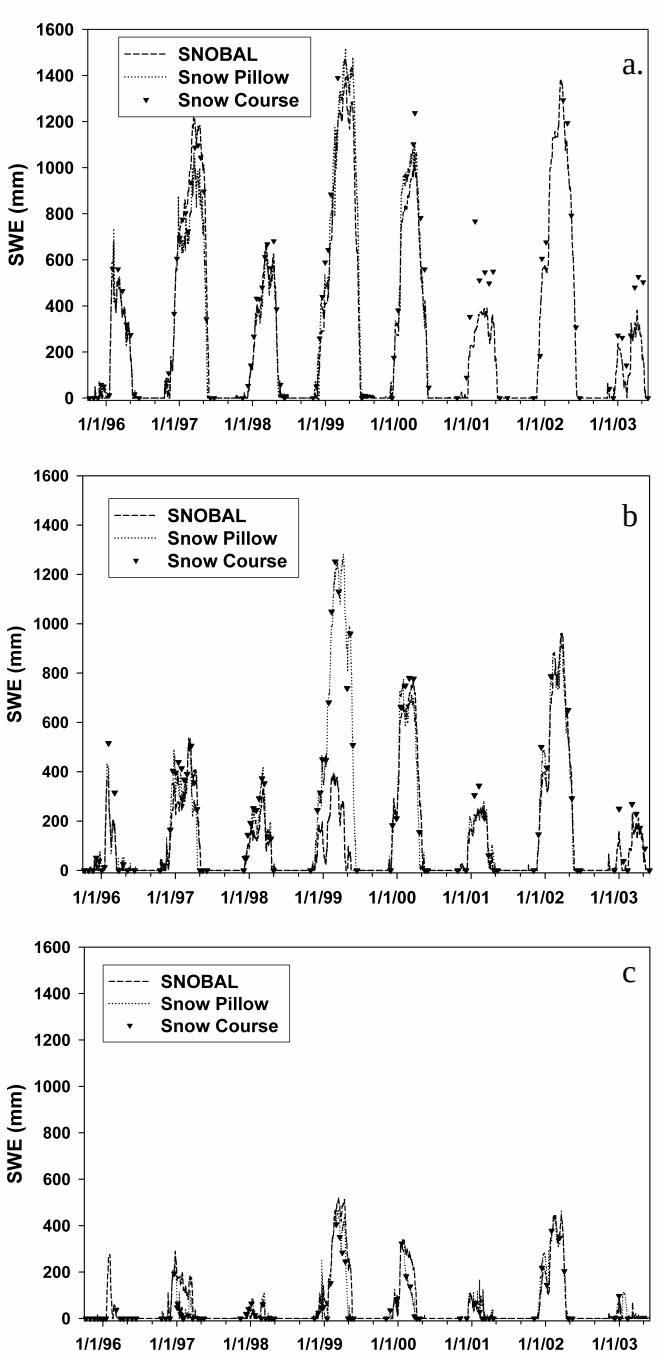

Figure 2.4 Modeled and measured SWE at UPLMET (a), VANMET (b), and CENMET (c).

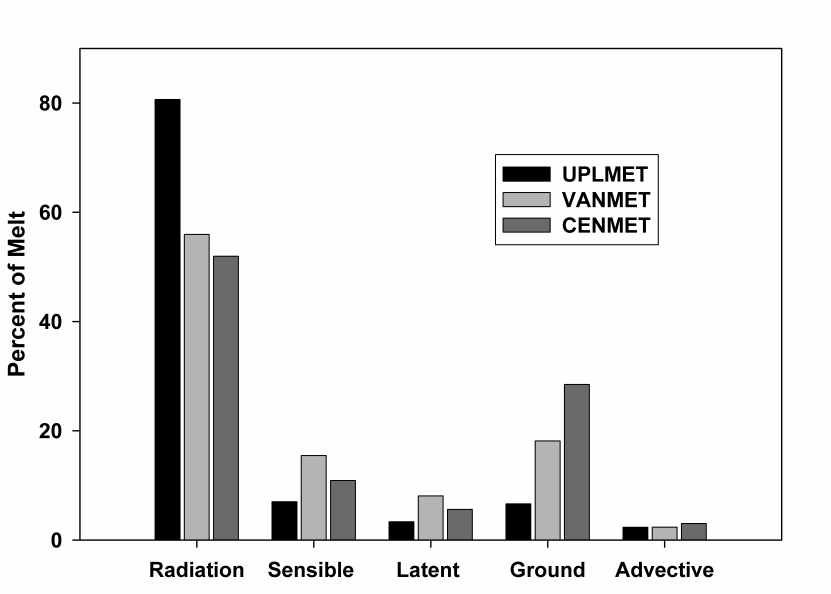

Figure 2.5 Modeled energy balance component contribution to total snowmelt at three sites, 1996-2003.

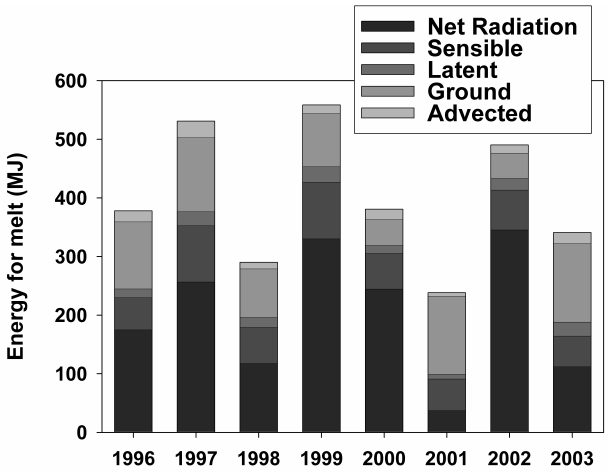

Figure 2.6 Annual energy balance components at UPLMET, 1996-2003.

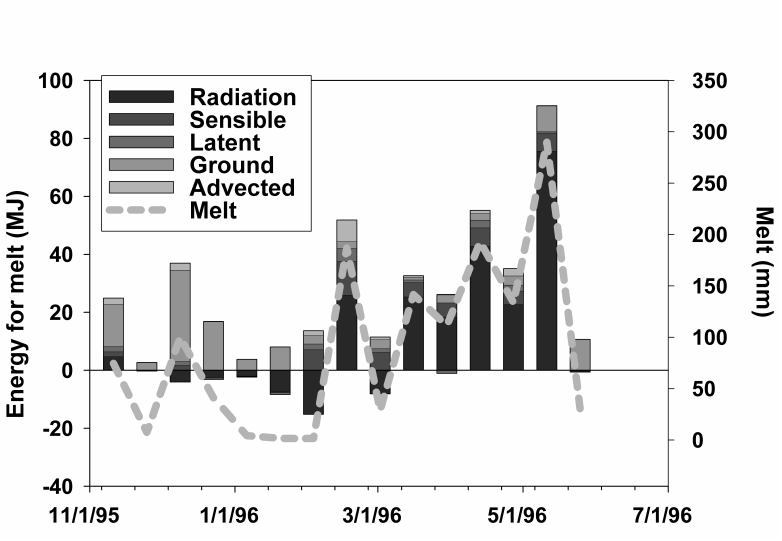

Figure 2.7 Energy balance components for 1996, biweekly timestep.

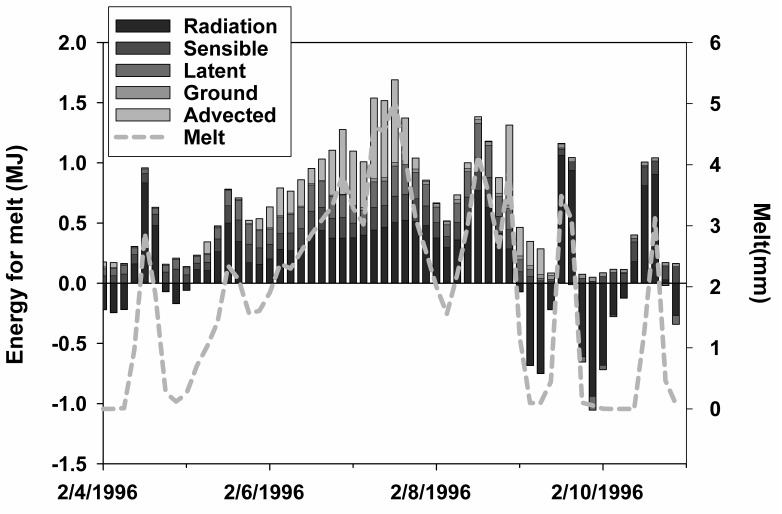

Figure 2.8 Energy balance components for ROS event, February 1996, 3-hour timestep.

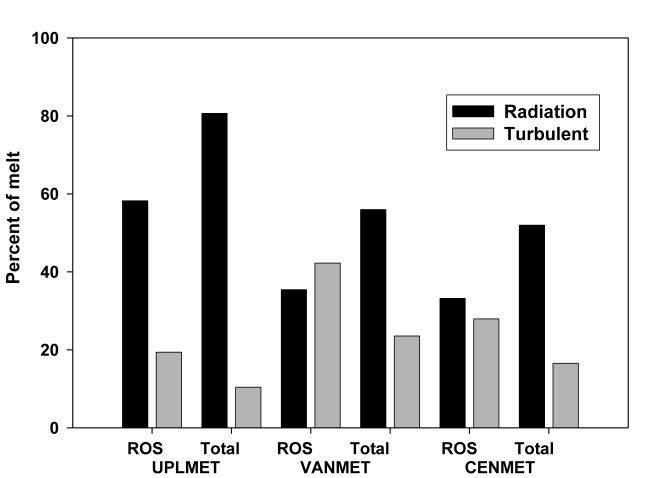

Figure 2.9 Modeled energy balance component contribution to snowmelt during ROS events at all three stations, 1996-2003.

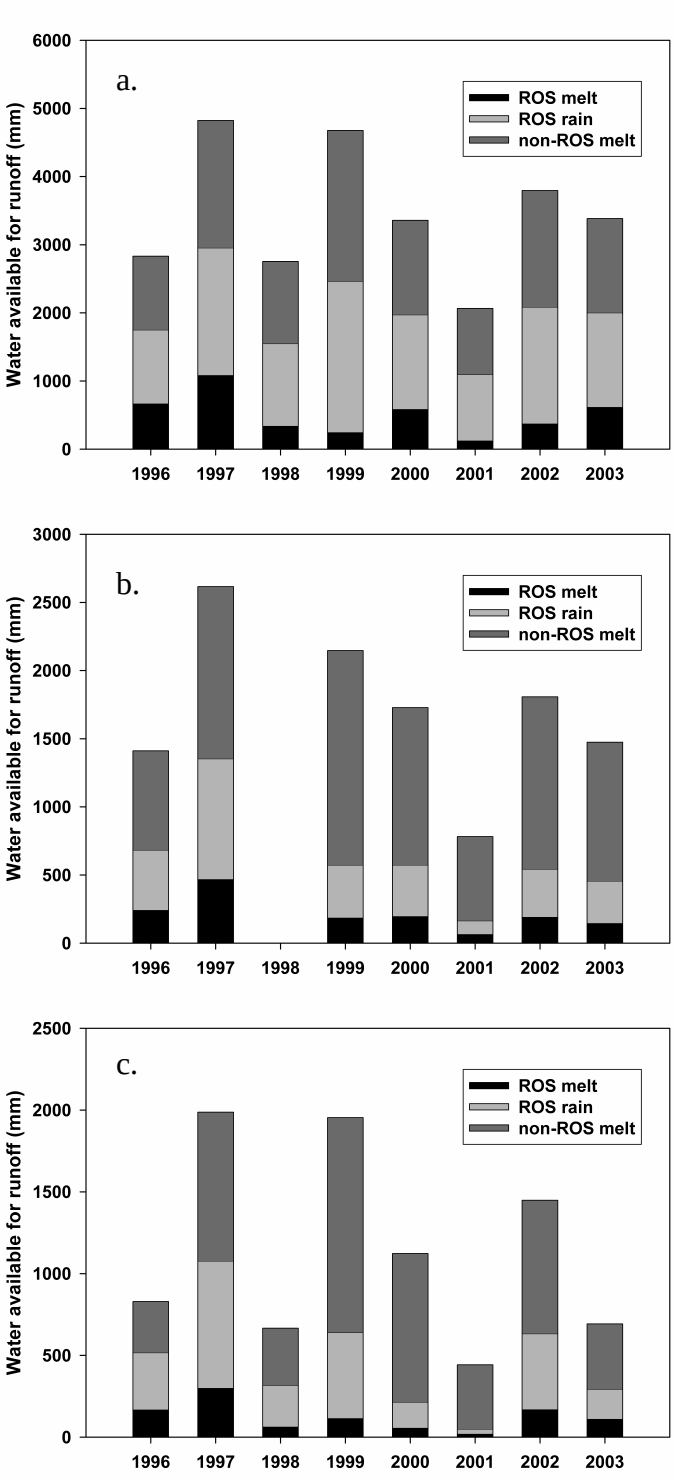

Figure 2.10 Water available for runoff derived from ROS events (rain + snowmelt) and non-ROS periods (snowmelt only) at UPLMET (a), VANMET (b), and CENMET (c)

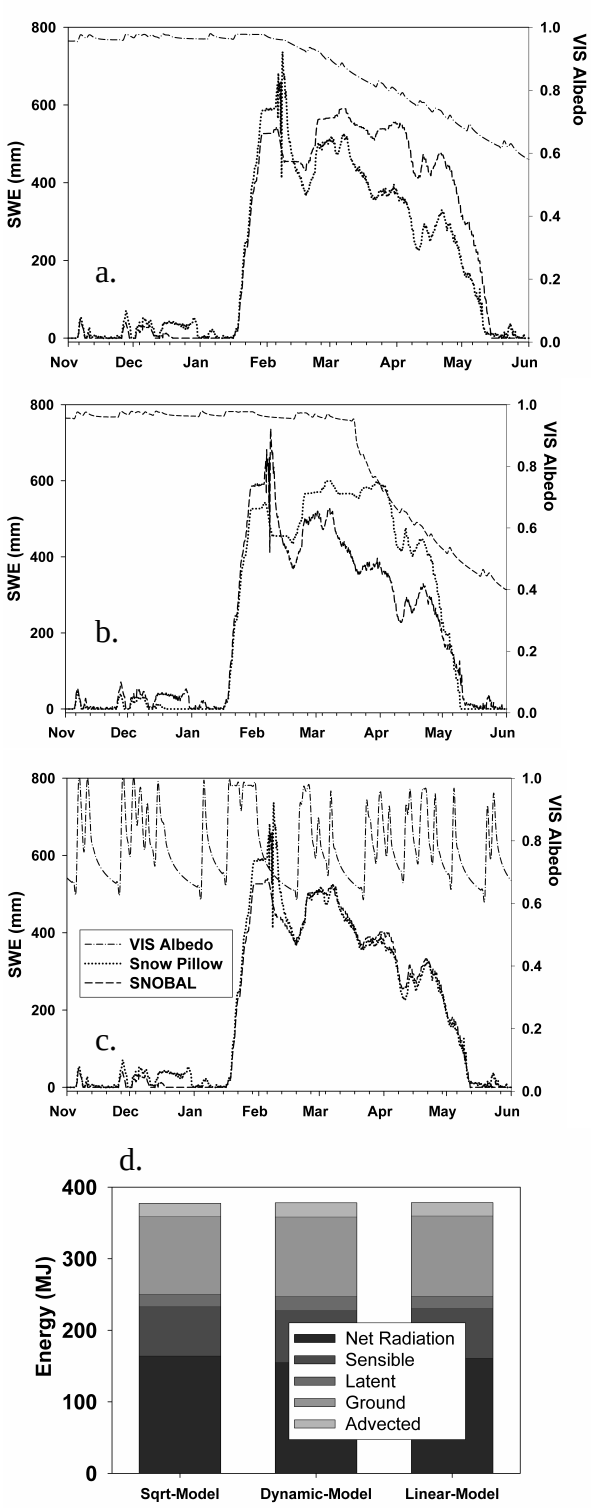

Figure 2.11 Energy balance components for WY 1996 for each albedo-reduction algorithm — linear decay (a), square root (b), dynamic (c), and annual EB for each function (d).

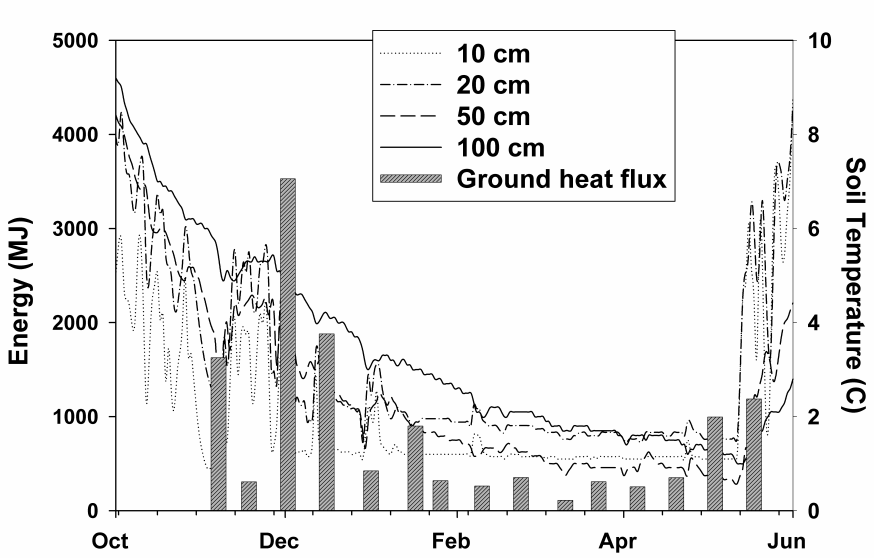

Figure 2.12 Soil temperatures at depth and ground heat flux for WY 1996

3 The effect of environmental change on watershed-scale snow regime: a virtual experiment approach

Mazurkiewicz, A.B.

McDonnell, J.J.

Garen, D.C.

Marks, D.

Woodsmith, R.D.

To be submitted to

Journal of Hydrology
Elsevier Inc., Amsterdam, Netherlands
in preparation

3.1 INTRODUCTION

The effects of environmental change (wildfire, land management, and climate change) on the snow regime at the watershed scale are poorly understood (Leaf and Alexander, 1975; Meiman, 1987; Storck et. al., 2002; Winkler et. al., 2005). In semi-arid watersheds of the Western U.S.A. snow can account for greater than 80% of annual streamflow (Marks et. al., 2002). Land managers in these snow dominated basins depend on the snowpack to act as their water supply reservoir for recharge through the spring melt season. Alterations to the snow hydrology of a basin will have an unforeseeable influence on watershed processes, streamflow generation, and resulting reservoir storage.

While environmental change will have an impact on catchment snow regime and the subsequent streamflow, predictions of these effects are problematic. In general regional-scale data analyses have shown that increases in average air temperatures will result in lower regional snow covered area (Nolin and Daly, 2006). Mote (2003) has linked changes in snow water equivalent (SWE) accumulation to increasing temperatures for data collected throughout the 20th century. Moderate warming over the next 50 years is expected to reduce mountain snowpack by as much as 60% in some regions of the Western U.S.A. (Service, 2004). An increase in average air temperature will increase the number of rain events during the winter, reduce regional snow covered area, and lead to an earlier spring melt regime (Mote, 2003). Warmer temperatures may result in continual melt throughout the winter, increasing winter streamflow, while lower snowpack accumulation will reduce peak spring streamflow and lengthen summer low flow.

Catchment based snow hydrology studies have linked snow regime patterns to streamflow measurements, while point scale investigations have used site comparison techniques to examine differences in snow accumulation and melt. Early studies, such as the Wagon Wheel Gap, found increases in streamflow and peak flow following canopy removal. However only broad conclusions about the effects of canopy removal on snow processes could be drawn (Van Havern, 1988). Troendle and King (1987) showed variable increases in snow accumulation and increased streamflow due to patch and clearcutting management techniques. Using point measurements, Winkler et. al. (2005) showed increased snow accumulation in a clearcut site compared to a thinned and a mature forest, where total seasonal accumulation loss in a clearing was twice as much as a mature forest. Golding and Swanson (1986) observed snow accumulation in forest openings to be 20% higher than in forested plots. While these field experiments have examined the influence of land management techniques on snow accumulation and melt, it is exceedingly difficult to measure the spatial distribution of snow energy balance (EB) components which create melt in complex terrain (Marks, 1992). Conversely, it is also difficult to regionalize point scale measurements over the watershed and meaningfully quantify change in a distributed way (Blöschl, 1999).

Recent modeling approaches investigating the effects of land cover change on watershed hydrology have focused on macro-scale watersheds (VanShaar et. al., 2002; Mote et. al., 2003). These studies have identified regions which contain 'at-risk snow' due to increases in average temperature (Nolin and Daly, 2006). These investigations have linked remote sensing and global circulation models to regional water supply to

assist with decision-making for municipal water supply, large dam regulation, and policy initiative. Watershed modeling studies in snow dominated basins, have focused on investigating the effects of environmental change on streamflow (Schnorbus and Alila, 2002; Seibert, 2006). Marks et. al. (2002) found local snow deposition patterns to be important in deciphering EB components. It has proven difficult to interpret and answer local land management questions that are affected by local changes in the snow regime. More problematic is the fact that catchment based modeling studies have been largely streamflow-based. Internal catchment storage and fluxes are a filter for the changes in snowmelt processes. Furthermore, water which makes up streamflow is often prior snow season precipitation (McGuire, 2005). In general, it has proven difficult to isolate the effects of the antecedent watershed condition and meteorological variability and their influence on the snow regime from streamflow-based analysis.

Investigating environmental change effects on water resources using field experiments is difficult. These investigations require intense measurements and are difficult to replicate over multiple seasons and over multiple vegetation treatments and climate regimes. Schnorbus and Alila (2004) were among the first to use a numerical simulation approach to generate random climate change scenarios within a watershed. The application of a model as a learning tool is an alternative way to classical field studies to examine changes in the snow regime. Loague et. al. (2006) argue that using physically-based models can provide a strong foundation for concept development. The application of physically-based models to develop new ideas and test hypotheses can increase our hydrologic knowledge base. This can be especially useful when we

use ‘numerical experiments with a model driven by collective field intelligence’ as advocated in the virtual experiment approach of Weiler and McDonnell (2004). Using this philosophy we can begin to understand how interactive processes will influence one another in a changing environment. In this study, we apply this philosophy to questions of snow hydrology and in particular to the ways in which snow energy balance components drive melt and water available for runoff (WAR) under different environmental scenarios in the Western U.S.A.

Our objective is to first reproduce the observed snowmelt patterns for water year 2006 in an experimental basin, located in Eastern Washington, U.S.A, using a physically-based snow energy and mass balance model, in order to identify the main energy balance components of snowmelt. We then ask this set of questions:

1) What are the main energy balance components of snowmelt?
2) How do these components vary with in space and time throughout the melt season?
3) How are snow energy balance components weighted in terms of melt amount produced?
4) How does environmental change — canopy removal, uniform forest canopy, and increases in average air temperature — affect spatial and temporal changes in the snow regime and energy balance components?

3.2 METHODOLOGY

3.2.1 Site Description

The 580 ha Burns Watershed is located in the Entiat Experimental Forest (EEF) on the East slope of the Cascade Mountains in Washington, U.S.A. A historical description of the EEF can be found in Helvey (1980) and Woodsmith et al. (2004). The EEF is a paired watershed experiment that was originally designed to investigate the effects of land management on watershed hydrology, geomorphology, and forestry. The East slope of the Cascade Mountains is characterized as semi-arid due to the rain shadow effect of the Cascade Mountain crest. The climatology is characterized by cool moist winters and dry, warm summers (Figure 3.1). Approximately 70% of the annual precipitation falls as snow (Helvey, 1980). The Burns watershed has a general south facing aspect, with steep slopes, averaging 50% (Helvey, 1980). The elevation ranges from 865 m at the outlet to 2150 m at the ridgeline. The catchment is within the Entiat River Basin, where a long-term watershed plan, which addresses water quality and quantity needs, has recently been completed (CCCD, 2004). The river is free flowing and the local economy depends on water for irrigation to support livestock and fruit orchards.

The vegetation in the Burns watershed varies in type and density, from relatively low-density mature Ponderosa Pine forests to dense successional forests of Douglas fir, Ponderosa Pine, and Alder (Figure 3.2). This patch work of forest cover reflects the regeneration of the forest since a severe wildfire in 1970. Prior to the fire, the watershed had a relatively uniform, mature forest canopy.

Meteorological data were collected at numerous climate stations during the 2006 field season (Table 3.1 and 3.2). Two snow pillow stations (Upper and Lower) have stainless steel snow pillows instrumented with Schaevitz Sensors Ultrastable 60 pressure transducers and Judd snow depth sensors. The lower pillow station also records air temperature using a Campbell Scientific 107-L thermistor and incoming solar radiation using LI-COR LI-200 silicon pyranometer. The Upper Snow Pillow station records air temperature using a Campbell Scientific 107-L thermistor. Four meteorological stations were used in conjunction with the snow pillow stations. The meteorological stations were instrumented with Onset weather stations recording air temperature, relative humidity, wind speed using cup anemometers, and wind direction. Field personnel also made snow survey measurements, using a Mt. Rose snow sampler, during winter maintenance at the Weir Met station and at the two snow pillow stations on November 11, February 22, and May 12.

3.2.2 Model - ISNOBAL

ISNOBAL is a physically-based snow energy balance model, developed (Marks et. al., 1992) and described in detail by Marks et. al. (1999a). The model has been successfully applied to the Boise River Basin (Garen and Marks, 2005), the Wasatch Range in Utah (Susong et. al., 1998), in the Boreal Ecosystem Atmosphere Study project (Link and Marks, 1999a), the California Sierra Nevada (Marks et. al., 1999a), and the Reynolds Creek Experimental Watershed in Idaho (Marks and Winstral, 2001; Winstral and Marks, 2002). A point version of the model has been applied to a number of locations including central Canada (Link and Marks, 1999b), Turkey (Sensoy et. al., 2006), and the Pacific Northwest (Marks et. al., 1998;

Mazurkiewicz et. al., in prep; van Heesjwick et. al., 1996). ISNOBAL is a utility built in the Image Processing Workbench (IPW) (Frew, 1990; Marks et. al., 1999b). The software operates in a UNIX environment with a command line interface. In addition to ISNOBAL, IPW utilities were used to calculate thermal radiation, relative humidity to vapor pressure conversions, clear sky solar radiation (Marks et. al., 1999b), and forcing data interpolations. UNIX scripts were written to execute the calculations.

3.2.3 ISNOBAL Forcing Data

The required forcing data for the model are distributed fields of net solar radiation, incoming thermal radiation, air temperature, precipitation, wind speed, vapor pressure, and ground temperature. These forcing data were processed at 1-hour intervals for each of the model runs.

3.2.3.1 Solar: The solar radiation (0.3-2.8 μm) modeling scheme followed Garen and Marks (2005) and Mazurkiewicz (in prep), which is a multiple step process that accounts for topography, albedo, surface debris, and atmospheric conditions. Point measurements of incoming solar at the Lower Snow Pillow station (Figure 3.2) were used as the benchmark for the radiation modeling and regionalization of cloud conditions. Clear sky conditions at the lower pillow were calculated using the IPW utility *twostream* for the sensor range (Table 3.1). The *twostream* model parameters were calibrated to 1200 PST clear day conditions for the modeling period at the Lower Snow Pillow. Incoming solar radiation was then calculated for October 1, 2005 to July 15, 2006. A ratio of measured solar radiation to clear sky modeled was then calculated to give a fraction of cloud cover. The cloud cover fractions for 1200 and

1300 PST were averaged to give a daily cloud cover factor. This point cloud cover factor was assumed to represent cloud cover over the entire basin.

Once the Lower Snow Pillow radiation model was calculated, the distributed calculations could be made using the parameters optimized at the point scale. First, potential incoming atmospheric solar radiation was corrected for cloud cover and separated for diffuse and direct components in both visible (VIS, 0.3-0.7 µm) and near-infrared (NIR, 0.7-2.8 µm) spectral ranges. The incoming solar radiation was then corrected for forest canopy effects on incoming solar radiation using an approach described by Link and Marks (1999a) to correct direct beam ($S_{b,o}$) and diffuse radiation ($S_{d,o}$). Direct beam radiation ($S_{b,f}$) was corrected as a function of canopy height (h):

$$S_{b,f} = S_{b,o} \times e^{-mh\sec(q)} \qquad \text{Equation 3.1}$$

where $S_{b,o}$ is beam solar radiation above the forest canopy, ? is the solar angle, and μ is the extinction coefficient. Diffuse radiation ($S_{d,f,}$) was corrected as a function of canopy transmissivity (t_d):

$$S_{d,f} = t_d \times S_{d,o} \qquad \text{Equation 3.2}$$

where $S_{d,o}$ is the diffuse shortwave radiation above the forest canopy and t_d is the transmissivity of diffuse radiation through the forest canopy. Parameters for t_d and μ (Table 3.3) were taken from Link and Marks (1999b).

Incoming solar radiation was corrected for topographic effects, such as shading and horizon effects using the IPW utility *toporad*. An albedo model was then used to correct for reflected radiation on a clean snow surface. Due to the accumulation of dust and debris on the snow surface and the cumulative exposure of debris throughout

the melt season, an albedo reduction calculation was used (Mazurkiewicz et. al., in prep). The albedo reduction (a_r) model:

$$a_r = 0.0607 * \ln(TimeSinceLastSnow) + 0.1398 \quad \text{Equation 3.3}$$

was applied starting on February 1. The albedo reduction model was applied until the lower limit of 0.7 for VIS and 0.4 for NIR is met.

3.2.3.2 Thermal Radiation: Thermal (longwave) radiation was estimated using techniques described in Mazurkiewicz et. al. (in prep) and Garen and Marks (2005). This technique is based on thermal radiation modeling developed by Marks and Dozier (1979). The algorithm accounts for topography and atmospheric conditions. Inputs to this model are elevation, vapor pressure, air temperature, and a sky view factor. The model does not account for increases in thermal radiation due to cloud cover. Garen and Marks (2005) developed a relationship between measured longwave radiation and measured shortwave radiation. The model was applied here to account for cloud coverage.

Thermal radiation (L_f) was adjusted for forested effects using (Link and Marks, 1999b):

$$L_f = t * L_o + (1 - t)e\,sT_v^{\,4} \quad \text{Equation 3.4}$$

where e is emissivity, s is Stefan-Boltzmann constant, t is transmissivity, L_o is above canopy longwave, and T_v is the vegetation temperature. This method applied the Stefan-Boltzmann equation accounting for emissivity and transmissivity of vegetation. The temperature of the vegetation was assumed to be air temperature, transmissivity of thermal radiation was assumed to be equal to t_s, and emissivity (e) to be 0.96 (Link and Marks, 1999a). Non-forested pixels had transmissivity of 1 and thermal

transmissivity of 0.75 was assumed for pixels which were defined as vegetation-free but had neighboring vegetated cells. The result was the modeled thermal radiation for ISNOBAL, accounting for location, cloud cover, vegetation, and atmospheric conditions.

3.2.3.3 Wind: Wind speed is a difficult parameter to both interpret and distribute over a spatial grid. Amplifying this difficulty is the existence of the forest canopy in complex terrain. An integrative approach was used to account for the forest canopy, wind direction, and topography. Three stations within the Burns basin were instrumented with anemometers: the Weir, 510Rd, and Frog Rx (Figure 3.2). These stations cover a range of elevation, aspects, and forest types. The Weir station is within a forest opening, resulting in wind speed measurements that are affected by the vegetation. Frog Rx and 510Rd are both relatively open stations. The 510Rd was open to all general aspects but is affected by a forest edge to the West, which was observed in the wind speed data. Frog Rx is protected to the North. These site characteristics made it difficult to extrapolate measurements beyond their measurement point.

Generally, wind speeds increase with elevation and should be a significant factor for snow accumulation and melt during storm events with high winds. The upper, exposed elevations received higher wind speeds. However, wind speeds were not consistent over each wind direction. Typical high wind speeds were measured from the South caused by low pressure systems. Measured wind speeds from the North were generally light, while the East and West winds varied in velocity. To account for all of these factors an integrative approach was taken to distribute wind

fields. First, to have the weir wind speed measurements comparable to Frog Rx and the 510 Rd, a forest correction factor of 1.8 was used (Link and Marks, 1999b). Next, wind speeds at each station for each general cardinal direction (North, South, East, and West) were averaged for the entire modeling period. These averages were then used to develop an elevational-lapse rate for each cardinal direction for the three meteorological stations. These lapse rates were applied across the basin from the 510Rd station for North, South, and East wind directions. Since the 510Rd was affected by a forest edge to the West, Frog Rx was used to model wind from the West.

Since topographic position affected wind speeds, an approach suggested by Ryan (1977) was taken:

$$W_F = \arctan(0.17V)/100 \qquad \text{Equation 3.5}$$

where W_F is the topographic correction factor for wind speed and V is the downwind horizon. The modeled wind speeds were then corrected for each wind direction using W_F. This took into account the surrounding downwind topography for each wind direction. The downwind horizon (V) was calculated in the IPW utility, *horizon*, and applied to the calculation.

The final step to model wind speed was to account for the vegetation. A canopy reduction factor of 0.2 (Link and Marks, 1999b) was applied to all forested pixels. In addition, the canopy correction was applied to an open pixel if a forested pixel existed in the direction of the wind.

3.2.3.4 Soil temperature: Soil temperature measurements were not made for the modeling period. However, field observations were made prior to the first snowfall, which indicated a frozen soil surface. During snow surveys, observations

were made of a thawed soil surface. From these observations we assume that the soil temperature was 0°C prior to the first snowfall and once the snowpack was established in the basin, December 1, 2005, a ground temperature of 0.2° C was assumed across the basin.

3.2.3.5 Air temperature: Air temperature measurements were made at Frog Rock, Upper Pillow, Lower Pillow, Waterfall, 510Rd, and the Weir. To spatially interpolate these data, a detrended kriging technique was used (Garen et. al., 1994). There were short periods of missing or questionable data due to difficulties with instrumentation. Elevational lapse rates were calculated for those time steps to estimate missing or flawed air temperature measurements.

3.2.3.6 Vapor Pressure: Relative humidity measurements were made at three stations: 510 Rd, Waterfall, and Frog Rx. While these three stations cover a broad range of the elevation, vapor pressure was found to be relatively uniform among these stations. The measurements were used to calculate an elevational vapor pressure lapse rate for each model time step. The lapse rates were then applied to the basin DEM to spatially interpolate vapor pressure. The vapor pressure images were then used to calculate dew point using the IPW utility *idewpt*

3.2.3.7 Precipitation: Precipitation records were not available for the winter period due to the lack of collection gauges. This required an estimate of precipitation record using SWE measurements from snow pillow data. Changes in daily SWE were calculated for the Lower Snow Pillow data. Increases in daily SWE were assumed to be due to a precipitation event during the snow accumulation period. This record was then compared to tipping bucket data to identify rainfall events that were missed by

the snow pillow estimation. Due to hourly data "noise" in the snow pillow data caused by sensor instability, it was not possible to estimate the time period within each day in which the precipitation fell. Pope Ridge SNOTEL site (approximately 12km, NNW from the basin) was used to determine the fraction of daily precipitation for each hour. A point simulation at the lower pillow was performed to evaluate the technique.

In order to interpolate the precipitation record over the basin we assumed that elevation controlled precipitation totals. We used an annual average precipitation estimate from PRISM (Daly et. al., 1994) to calculate an elevation lapse rate of annual average precipitation. We assumed that this lapse rate applies to all precipitation events and applied the lapse rate to each hour's precipitation record. Dew point temperature was used as a proxy for precipitation temperature, type, and density (Marks et. al., 1999b) (Table 3.4).

3.2.4 Interception Model

ISNOBAL does not account for precipitation interception in the forest canopy. This can be important if there are large losses of intercepted snow to evapo-sublimation. In order to account for these processes, a snowfall interception model was developed utilizing tools in IPW**.** The interception model was structured following the Distributed Hydrologic Soil and Vegetation Model (DHSVM) approach as described in Storck et. al. (2002). The routine is a physically-based approximation, in which snowfall is intercepted at a predefined efficiency rate with a maximum holding capacity. Precipitation falling as snow is assumed to be intercepted at a fixed efficiency of 40%, until the canopy storage capacity of 40 mm is met or exceeded.

Once the storage capacity was met, additional precipitation resulted in direct throughfall to the forest floor. An energy balance is then calculated for the intercepted snow to estimate melt. If melt occurs, evapo-sublimation was assumed to occur at the potential rate. Melt from the forest canopy, resulted in throughfall at 0°C. An unloading factor is used to account for loss of intercepted snow caused by mass unloading of branches. An unloading factor of 0.4 is assumed (Storck et. al., 2002).

3.2.5 Model Runs

3.2.5.1 Climate Change Scenario

To investigate the effects of climate change on the snow regime, two climate change scenarios were modeled. The climate change scenarios followed the estimated temperature increase for the years 2020 and 2040, 2.7°C and 4.1°C (CIG, 2004). To model these scenarios, we increased the air temperature for each time step by 2.7°C and 4.1°C and held relative humidity to measurements made in WY 2006. With the increase in air temperature, we re-calculated thermal radiation, vapor pressure, net solar radiation, and precipitation inputs (Table 3.5) for each model run.

3.2.5.2 Land Coverage Change

Two scenarios were modeled to investigate how land cover change may affect catchment snow regime. The first scenario was 100% canopy removal (vegetation free) across the entire basin. The second is a 100% uniform canopy over the entire basin. In order to represent these landscape changes, the forcing data were adjusted to represent the new land cover (Table 3.5). In both scenarios thermal radiation, net solar radiation, and wind speed were adjusted to account for the forest cover effects. The

removal of the forest canopy simplified the precipitation modeling scheme presented earlier by negating the need for an interception module. The net solar, thermal radiation, and wind speed parameters are not corrected for forest cover.

In order to represent a 100% uniform canopy, we defined the canopy height of 30m and a canopy density of 50%. This is representative of forest conditions as reported by Helvey et. al. (1976). The meteorological forcing data that were adjusted are net radiation, thermal radiation, wind speed, and precipitation. The parameters for the shortwave and thermal radiation scheme are shown in Table 3.3. Wind speed was corrected for forest cover across the entire basin as described earlier.

3.3 RESULTS

3.3.1 2006 Model Run

Model results from the 2006 field season matched well with measurements within the basin (Figure 3.3). The Nash-Sutcliffe coefficient for the Lower Snow Pillow for daily change in SWE (200 days) was 0.97. Calculations were made at 2400 PST on each day to bypass "noise" present in snow pillow measurements caused by daily heating of the transducer enclosure. The model followed the accumulation and melt period measured by the lower snow pillow closely (Figure 3.3). The model calculated a melt out three days earlier than what was measured by the snow pillow. Field visits indicated that there was patchy snow cover at mid-elevations within the Burns watershed prior to snow pillow melt out.

The measured Upper Snow Pillow (Figure 3.3) did not match the accumulation pattern of the Lower Snow Pillow or nearby Pope Ridge SNOTEL station

measurements. We interpret this as faulty snow pillow measurements. The lack of measured accumulation at the Upper Snow Pillow during March (Figure 3.3) suggests that snow bridging occurred during the month of February, when the weather was mostly clear and dry. Snow survey measurements at the Upper Snow Pillow indicate the model produced reasonable results for the upper elevations, tracking the snow accumulation period. These ancillary data and snow patterns from the surrounding stations, supports the notion that ISNOBAL produced reasonable results for the Upper Snow Pillow portion of the Burns watershed.

A comparison of ISNOBAL estimates of snow depth and snow depth measurements from the Weir station showed a reasonable pattern of snow accumulation at the lower elevations (Figure 3.4). The initial modeled accumulation period to the February peak and the modeled melt out timing coincides with field-based snow depth measurements. The February dry period did show a discrepancy between the modeled and measured snow depth. We interpret these errors as attributed to inaccurate snowpack density estimates.

Oblique basin-wide photographs were taken during the spring melt period to track snow covered area (SCA). The approximate snowlines are shown as white lines for April 25 and May 9 in Figure 3.5. These data indicated a relatively fast retreat of the snowline in the two week time period between photos. While a rapid retreat in SCA was shown by the model, the snow line pattern demarcation did not match perfectly with the photographs. The model predicted snow to exist at lower northwest elevations while photographic data showed all of the lower elevations to be snow free. This may be due to inaccurate parameterization of vegetation parameters in the

radiation modeling or misclassification of vegetation in the survey data. These discrepancies notwithstanding, the general pattern of rapid melt-out of the south facing slopes was captured by the model output (Figure 3.5).

3.3.2 EB Components of the 2006 Model Run

Radiation dominated the snow energy balance at the Burns Watershed (Figure 3.6). At the Upper Snow Pillow, radiation accounted for 77% of the energy available for melt during SWE loss. At the Lower Snow Pillow radiation (Figure 3.6) accounted for 98% of the energy during snowmelt. These high percentages of radiation input indicate that the solar radiation was the most important input to melt within the Burns catchment.

Sensible heat flux also played an important role in causing snowmelt in the upper basin. During active melt, 22% of the EB was comprised of sensible heat inputs at the Upper Snow Pillow, compared to only 1% at the Lower Snow Pillow. This high variability appeared to be due to differences in wind speeds. The Upper Snow Pillow was much more exposed and susceptible to higher wind speeds, due to its topographic position. The surrounding vegetation at the Lower Snow Pillow reduced wind speeds.

Patterns of high radiation inputs to melt across the basin are shown in Figure 3.7. Generally, south-facing slopes showed lower net radiation inputs to the overall EB for the entire year compared to other areas of the basin due to high sensible heat exchanges in this zone throughout the snow year. The south slopes maintained little vegetation that allowed for higher wind speeds and subsequently high mid-winter sensible heat exchanges. High sensible heat exchanges throughout the year caused earlier melt-out timing in the spring, before high solar insolation days.

Temporal variability of snow energy inputs (Figure 3.7) reflected the seasonal cycle of the solar radiation. Significant melt was delayed until high radiation inputs were available that are caused by high sun angles and longer duration of solar insolation. Early season spatial EB components showed a net radiation loss early in the winter, due to short days and longwave cooling. Latent heat flux early in the season was also a positive contributor to melt due to cool snowpack temperatures and high air humidity. This created a vapor pressure gradient into the snowpack, resulting in condensation flux into the snowpack. As the spring melt season progressed, radiation became an important input to the EB, while the warmer, dry air caused a net loss of latent heat and an increase in sensible heat flux (Figure 3.7). The upper NW forest area of the basin showed low to negative sensible heat exchanges throughout the spring melt. This was due to low wind speeds under the forest canopy. Ground heat fluxes were positive throughout the year due to a negative temperature gradient between estimated soil temperatures and snowpack temperature.

We used a weighting approach to identify the importance of each of the EB components in creating water available for runoff (WAR):

$$M_{ec} = E_c \div Q_m * M \qquad \text{Equation 3.4}$$

where M_{ec} is the weighted EB components for WAR, E_c is amount of energy an EB component positively contributes, Q_m is the total positive energy for melt, and M is the amount of WAR. These results were comparable to EB components. Radiation created a high percentage of WAR across the basin (Figure 3.8). Radiation caused a majority of WAR at the upper and lower pillows (81% and 93%), while sensible heat inputs accounted 17% and 3% of the WAR.

3.3.3 2020 & 2040 Model Scenarios

Increases in average air temperature affected the amount of snow accumulation, the timing of melt, and the EB components of melt and WAR. Snow accumulation patterns for the modeled scenarios (Figure 3.9) showed distinct differences from the 2006 model simulation. Peak basin snow accumulation for 2020 (Table 3.4) was 158 mm/m^2 and 94 mm/m^2 for 2040. The date of peak accumulation for 2020 was February 8; 6 weeks earlier than the 2006 simulation. Peak snow accumulation for the 2040 scenario was greatly accelerated and occurred 1.5 months earlier than the 2006 model simulation. Melt in both of the increased temperature scenarios, resulted in the basin-wide melt out earlier in the season (Figure 3.9).

Radiation dominated components of the EB for both the 2020 and 2040 modeling scenarios (Figure 3.6). The warmer temperatures during the modeled winter created more melt throughout the year and also resulted in fewer snow events. Sensible heat fluxes at the Upper Pillow were 32% of energy towards melt for the 2020 scenario, and 37% for 2040 scenario. These additional energy contributions caused shorter overall snow seasons in each case. The shorter snow season resulted in lower positive radiation inputs over the entire snow year because the snow was not subject to the high radiation inputs of the later spring.

The seasonal patterns of the EB inputs in the climate change scenarios are shown in Figures 3.10 and 3.11. Radiation inputs were high at both the Upper and Lower Pillow sites when a majority of the melt occurred. During periods of high melt in the spring, large negative latent heat fluxes were absent. This was caused by low vapor pressure gradients between the snow surface and the atmosphere. Peak melt at

the Upper Snow Pillow for the 2020 scenario did not show a shift in timing, but did show an increase in peak melt magnitude of 15% (Figure 3.10). The Lower Snow Pillow showed an abrupt change in peak melt timing and magnitude for both climate scenarios (Figure 3.11). Peak melt occurred approximately one month earlier in the 2020 scenario and approximately two months earlier in the 2040 scenario.

Increases in temperature for the two scenarios resulted in higher sensible heat contribution to WAR (Figure 3.8). Nevertheless, high radiation inputs to the energy balance generated the greatest amount of WAR overall. Both the upper and lower pillow station's WAR regime were dominated by net radiation in both climate scenarios (Table 3.6). Net radiation contributions decreased with the increasing temperatures.

3.3.4 Land Cover Change Model Scenarios

Meteorological conditions of 2006 were used while vegetation parameters were adjusted to model land cover change scenarios. Land coverage change had a large effect on basin snow accumulation and melt regime. The overall basin snow accumulation and melt in the vegetation-free scenario (Figure 3.12) showed a slightly lower SWE peak (Table 3.6) compared to the status quo 2006 model run. The 100% vegetation model run showed approximately 1.5 month delay in the melt regime in comparison to the vegetation free and 2006 model runs. Peak SWE was delayed by 3 weeks while melt out was delayed by one month.

Mid-winter WAR (Figure 3.12) during the vegetation-free scenario was lower, however spring melt daily peaks were much higher and flashier than the 2006 model run (Figure 3.12). This was caused by high inputs of daily direct-beam radiation on

the open slopes (Figure 3.8). The annual WAR pattern was similar to the 2006 model run, with melt commencement in late March and leveling off in late April (Figure 3.12). These modeled WAR patterns differed greatly from the forested version model run. The 100% vegetation model run melt and WAR were delayed until late April. The timing of the WAR initiation coincided with the end of WAR during the 2006 and cleared model runs.

The 100% vegetation model run showed a very different melt cycle from the 2006 season. Radiation inputs were low throughout the winter and spring (Figures 3.10 and 3.11). Spring melt did not begin until solar angles were high, allowing shortwave radiation to penetrate the forest canopy. Wind speeds were low within the forest resulting in low turbulent exchanges. Melt rates and amounts were low due to the low energy inputs; this caused a more protracted melt and a longer snow covered season (Figure 3.12).

3.4 DISCUSSION

Studies that examine how environmental change influences the snow regime have shown variable effects. Winkler et. al. (2005) reported increases of 5-70% of snow accumulation in forest clearings. The typical setting for these investigations is within paired watershed studies, which often use streamflow as a proxy for melt dynamics. These studies use pre- and post-treatment study techniques (Troendle and King, 1985) or site comparison between forested sites and clearings (Winkler et. al., 2005). Both of these study techniques are subject to meteorological variability and inconsistent antecedent conditions which may interfere in the extrapolation of

conclusions to generalizations. A comparison between two different locations may be influenced by meteorological variability within the basin. A major factor in these studies is the position of each sampling site relative to dominant wind direction (Gary, 1974). While the field investigations have given the field of snow hydrology a strong basis to make inferences about the interactions of forests and the snow regime, it is not clear when generalizations apply. More importantly, the runoff dynamics and subsurface storage filter the cumulative environmental change effects.

The development of physically-based snow energy balance models and the parameterization of vegetation components (Link and Marks, 1999a and 1999b) allow us to remove the variability of the meteorological components and antecedent conditions to reasonably decipher the processes which control the melt regime. Once the dominant factors of the EB are described, the effects of environmental change scenarios can be isolated and examined. Climate and land use changes will impact the snow regime in both accumulation and melt periods. Climate change studies have shown consistent results of rising snowline elevations in regional studies (Mote et. al., 2003; Mote, 2003). In the PNW this will result in a vast reduction in the volume of water stored as snow (Nolin and Daly, 2006). Changes in snow covered areas and the rise of the snowline will impact the timing of streamflow and melt of the existing snowpack. Local land managers which plan water use and allocation based on current snowpack conditions will face unpredictable changes in water resources. As with climate change, an alteration in land cover due to land management or fire will have a distinct impact on snow accumulation and melt. These environmental changes will

have local and regional impacts, which affect water allocation, dam regulation and aquatic habitat (Mote et. al. 2003).

While inferences can be drawn on how environmental change will affect the snow regime based on streamflow analyses, identifying and understanding the EB components within the study area will link the cause and effect of snowmelt processes. Marks et. al. (1998) showed strong differences in EB components between a forested and cleared site during a major storm event. They found high rates of turbulent exchange in an open site which were driven by high wind speeds. This single event study showed the spatial variability of EB components within a single watershed. It would be inferred from this work that created forest openings would be more susceptible to high turbulent exchanges. Understanding the EB components lends us information on the trajectory of the effects of environmental change on the snow regime.

3.4.1 2006 Field Season

ISNOBAL was able to simulate water year 2006 and we found that radiation dominated EB components across the basin (Figure 3.8). Temporal variability of the primary EB components at the two snow pillow sites reflected inputs at different times of the season. In the winter and early spring, turbulent exchanges were increasingly important, where as beginning mid to late spring net radiation became a progressively dominant contributor of energy for melt. Winstral and Marks (2002) found similar results of increased contribution of radiation components to melt. In both cases high solar angles of late spring caused peak melt conditions. Spatial variability of input components within the basin showed that the lower elevation south facing slopes have

lower net radiation inputs to the EB over the entire snow year. This is counterintuitive, in that we would expect that the south facing, open slopes would have high radiation inputs in comparison to upper elevation north facing slopes. However, it appears that turbulent exchanges do play an important role in the EB in these areas of the basin. Where shallow snowpacks are exposed to winds, turbulent exchanges are steady throughout the winter period which is reflected in the annual EB.

The variability of turbulent fluxes across the Burns basin was largely controlled by topographical position and vegetation. The Upper Snow Pillow station showed the highest sensible heat inputs to snowmelt, while the Lower Snow Pillow had relatively low sensible heat exchanges. The Upper Snow Pillow's position near the ridgeline resulted in susceptibility to turbulent exchanges. Investigations at the Reynolds' Creek Experimental Watershed also showed great spatial variability of turbulent exchange components throughout the basin (Marks and Winstral, 2001). Sensible heat exchanges at an upper elevation ridge site were approximately 5 times that of a sheltered site during melt out (Marks and Winstral, 2001). In the Burns basin we found nearly the same results with sensible heat exchanges at the Upper Snow Pillow accounting for approximately 5.5 times more WAR than sensible heat exchanges at the Lower Snow Pillow. We interpret this difference as due to the position of the Lower Snow Pillow site — well protected by topography and surrounding forest from wind.

3.4.2 Environmental Change Scenarios

The importance of individual EB components changed in the environmental change scenarios when compared to the 2006 EB components and distribution. There

was an increase in sensible heat exchange in the annual EB for the two snow pillow stations in the increased air temperature climate change scenarios. This reflects the warmer air temperatures which caused a higher temperature gradient resulting in greater sensible heat exchange. The general decrease in annual inputs of radiation reflects a shorter snow season, where melt out occurs before the high solar insolation days of the late spring. The average temperature increase scenarios shifted the melt cycle and EB processes to earlier in the season at both snow pillow sites. Biweekly melt sums for each site are lower in these scenarios. This is because sensible heat transfers are not efficient during average wind speeds and incoming radiation is relatively low due to low solar angles. However, radiation inputs still dominate the snowmelt EB.

The land use change scenarios showed different results at each of the snow pillow sites. The Lower Snow Pillow showed a decrease in net radiation for the cleared model run which was caused by higher magnitude sensible heat exchange during melt. While shortwave radiation was similar to the 2006 model simulation, increased sensible heat exchanges were due to higher wind speeds. This resulted in an overall increase in turbulent exchange as a percentage of the EB. Link and Marks (1999a) showed high late season radiation inputs in forested areas during melt compared to an open site which had higher turbulent fluxes. During melt, their open site had lower magnitude net radiation inputs. Link and Marks (1999a) reported that melt occurred at the open site approximately four weeks earlier than the forest sites. Our results are very similar to Link and Marks (1999a) for the Burns Basin.

The forested model run at the Burns Lower Snow Pillow showed a decrease in net radiation over the annual energy budget. This is attributed to the presence of vegetation blocking incoming shortwave radiation (Figure 3.6). Calculations of incoming solar radiation are highly dependent on forest height and solar angle (Equation 3.1) (Link and Marks, 1999a). This delays high solar radiation inputs until the solar angle is high allowing shortwave radiation to penetrate the forest canopy. Solar angles reach these zenith angles late in the spring which cause increased melt rates throughout the basin.

Sensible heat exchanges were most affected by reduced wind speeds at the Upper Snow Pillow site during the forested model run. The surrounding vegetation restricted wind speeds, reducing the sensible heat exchange. This reduction in sensible energy exchange compares well with numerous studies that have shown increased sensible heat exchanges at open sites (Berris and Harr, 1987; Marks et. al. 1998; Marks and Winstral, 2001).

The model results showed that decreases in snow accumulation affected the importance of each EB contributor. Snow which exists in late spring and early summer season is subject to high solar radiation, which increases the overall percentage of net radiation inputs to melt. A shallower snowpack causes a shorter snow season and radiation becomes a lower overall annual energy contributor. The shorter season snow is then affected by sensible heat fluxes that occur throughout the winter. Numerous studies have shown that vegetation cover and topographic position greatly affect the snow regime (Marks et. al., 2002; Pomeroy et. al., 2003) with elevation being a major influential factor (Meiman, 1987). The variation in snow

patterns in the Burns modeling runs reflects these factors in the SWE estimates across the basin. The addition of 100% vegetation shows the potential of a four-week longer snow covered season and a delayed melt season. The modeled accumulation period was similar to the 2006 run because there was little loss of snow to evapo-sublimation. At the Lower Snow Pillow a net loss of sublimation of 7.5 mm was calculated for 2006, while the vegetation-free scenario a net gain of 16 mm was modeled. The gain of water in the vegetation-free scenario indicates that high wind speeds coincided with high atmospheric vapor pressure. The lack of evapo-sublimation from the forest canopy resulted in the majority of the intercepted snowfall reaching the ground as throughfall and melt water, or through mass unloading. Vegetation reduced radiation and turbulent exchange throughout the winter. This is comparable to Winstral and Marks (2003) who showed increased snow accumulations in sheltered areas of their basin. The 100% vegetation cover scenario caused a protracted peak SWE and delayed melt. This again is consistent with to the Winstral and Marks (2003) study site, where vegetation greatly influenced wind speed and snow redistribution processes

Changes in the melt regime from temperature increases caused the Burns basin SWE values to become greatly reduced and the timing of melt out to occur earlier in the snow year (Figure 3.12). This coincides with climate change simulations of snow covered area for the Pacific Northwest (Mote et. al., 2003). Mote et. al. (2003) showed a significant reduction in regional low elevation snow for 2020 simulations, while a 2040 simulation caused regional snow melt patterns to advance to a month earlier than the base model. Annual cumulative basin WAR for our model scenario suggests that soil water inputs would be continuous throughout the winter caused by

snow to rain event conversion, due to temperature increases and by mid-winter melt events.

3.4.3 Hotspots for snow regime change

Our modeling scenario approach can help to identify areas of the Burns watershed that are *hotspots for snow regime change* (McLain et. al., 2003). Understanding where, why, and how watershed areas are most sensitive to change is important for answering both land management and climate change questions. Accumulation maps (Figure 3.9) show the differences of SWE patterns between the 2006 and environmental change scenario model runs. South-facing slopes, which are most exposed to radiation and wind, have the most variability in SWE between the modeling scenarios and water year 2006. The increase of sensible heat exchange in this area, whether it is caused by increased wind speeds or greater snow-atmosphere temperature gradients, resulted in melt throughout the winter and in lower peak SWE. High elevation, NW aspects are protected from both wind and radiation, resulting in the longest snow covered periods. In other studies, south facing slopes have been found to hold less snow and be more susceptible to melt events. Pomeroy et. al. (2003) showed south facing slopes contained about 20-25% less snow covered area throughout the winter season. At Burns, these slopes showed a higher variation in percent snow covered throughout the study period and were susceptible to melt events throughout the winter.

The south-facing slopes of Burns watershed are sensitive to change. The 2006 model run depicted this area as mainly vegetation free; however, these slopes have not yet recovered from a wildfire in 1970. The forest conditions represented in our 100%

vegetation model run would be comparable to pre-1970 wildfire conditions. When the slopes of the basin are vegetated, melt became delayed to late spring, while the loss of vegetation resulted in faster melt and even earlier melt-out in the climate change scenarios. The removal of vegetation on these susceptible slopes coupled with an above average snow year would result in streamflows as reported in Helvey (1980) for the Burns basin.

3.4.4 Outstanding Modeling Issues

Shifts in EB components that control snowmelt are impossible to predict without the use of a physically-based model. The application of ISNOBAL to the Burns watershed showed distinct increases in turbulent energy exchanges in climate change scenarios. Nevertheless, radiation remained the dominant input to melt. Conceptually based snowmelt models, such as temperature index models would not be able to capture these shifts in the EB components — causing conclusions to be based on model runs which are right for the wrong reasons. Climate and land cover change modeling studies which employ temperature index models are calibrated to current and measured conditions, then apply the parameters to a new model scenario. Modeling trials using a temperature index model for the Burns basin showed very different results than was found using the EB approach (Figure 3.3). The shift in the melt regime followed the change in the temperature pattern. The dominance of net radiation and sensible heat exchanges to melt in this study and those reported elsewhere (Link and Marks, 1999a; Marks and Winstral, 2001; Pomeroy et. al., 2003) show that highly interactive components of the EB are poorly defined by a simple melt factor equation.

In order to reduce uncertainty in process-based modeling, additional field investigations are necessary to identify the interactions of forest cover on the EB components. Since net radiation has proved to be the most important factor in creating melt, evaluation of forest parameters and their effects on solar radiation attenuation and thermal radiance is needed. Hardy et. al. (2004) have shown vegetation temperatures to be higher than measured air temperatures throughout the day. However, accurate routines to estimate vegetation temperatures are not yet available. Also, solar radiation inputs greatly affect snowmelt rates. Albedo measurements below a forest canopy are needed. To date, few studies if any have developed a useful estimate of below canopy snow albedo. We used a decay function to estimate the evolution of surface debris which reduces the snow surface albedo (Garen and Marks, 2005; Link and Marks, 1999; Mazurkiewicz et. al., in prep). Future work is needed to validate and improve this approximation.

3.5 CONCLUSIONS

Radiation inputs accounted up to 98% of the energy creating WAR in WY 2006. This value is higher than estimated by Marks and Dozier (1992) (approximately 75%) at an alpine lake site. This large contribution of energy dominated EB for melt in the climate change and land cover change modeling scenario as well. Forested model runs also indicated high radiation inputs in creating WAR due to longer snow seasons which receive early summer solar insolation. The annual percentage of sensible heat contributions increased 4-5% during the shorter snow seasons in the 2020 and 2040 model simulations. Sensible heat exchanges were positive throughout

the winter and caused melt during the winter. Removal of the forest canopy increased turbulent fluxes in the basin which were influenced by vegetation. The percent of WAR attributed to sensible heat flux at the Lower Snow Pillow increased by 10% due to canopy removal.

The dominance of radiation in the EB dictated the areas of a basin that were most susceptible change. South slopes which had the most exposure to radiation and susceptibility to high wind speeds were the most affected by increases in air temperature and changes in vegetation cover. Vegetation reduced wind speeds and attenuated solar radiation inputs, which greatly increased annual snow accumulations. Warmer air temperatures caused higher snow-atmosphere temperature gradients increasing sensible heat exchange contribution to melt throughout the season.

3.6 ACKNOWLEDGEMENTS

The authors would like to thank Danny Marks, for his help in running ISNOBAL, David Garen for his guidance in creating distributed forcing data. Rick Woodsmith and Pamela Wilkins assisted with collection the meteorological and snow survey data. David Alley is thanked for his help installing and maintaining stations. Melissa Webb is also thanked for helping with installation of snow pillow stations. Snow survey assistance was provided by Scott Pattee and Bill Overman. A critical manuscript review by Anne Nolin is greatly appreciated. This study was funded by the USDA Forest Service under the contract PNW 03-CA-11261921-529 - *Processes of Water Cycling and Streamflow Generation in Semi-Arid Watersheds in Eastern Washington-Understanding Landuse Effects on Water Quantity and Quality.*

3.7 REFERENCES

Berris, S., Harr, R.D., 1987. Comparative snow snow accumulation and melt during rainfall in forested and clear-cut plots in the western Cascades of Oregon. Water Resources Research 23, 135-142.

Blöschl, G., 1999. Scaling issues in snow hydrology. Hydrological Processes 13, 2149-2175.

Chelan County Conservation District (CCCD), 2004. Entiat Water Resource Inventory Area(WRIA) 46 Watershed Management Plan. Electronic document available on Internet at http://www.chelancd.org/WRIA46_Plan.htm

Climate Impacts Group (CIG), 2004. Overview of climate change impacts in the U.S. Pacific Northwest. University of Washington, Seattle, WA. Electronic document available on Internet at www.cses.washington/edu/cig.

Christensen, N.S., Wood, A.W., Voisin, N. Lettenmaier, D.P., Palmer, R.N., 2004. The Effects of Climate Change on the Hydrology and Water Resources of the Colorado River Basin, Climatic Change 62 (1), 337-363.

Daly, C., Nelison, R.D. Phillips, D.L., 1994. A statistical topographic model for mapping climatological precipitation over mountainous terrain. Journal of Applied Meteorology 33, 140-158.

Frew, J., 1990. The Image Processing Workbench. PhD Thesis, Department of Geography, University of California, Santa Barbara, CA, pp. 382.

Garen, D.C., Marks, D., 2005. Spatially distributed energy balance snowmelt modeling in a mountainous river basin: Estimation of meteorological inputs and verification of model results. Journal of Hydrology 315, 126-153.

Garen, D.C., Johnson, G.L., Hanson, C.L., 1994. Mean areal precipitation for daily hydrologic modeling in mountainous regions. Water Resources Bulletin 30(3), 481-491.

Gary, H.L., 1974. Snow accumulation and snowmelt as influenced by a small clearing in a Lodgepole Pine forest. Water Resources Research 10(2), 348-353.

Golding, D.L., Swanson, R.H., 1986. Snow distribution patterns in clearing and adjacent forest. Water Resources Research 22(13), 1931-1940.

Hardy, J.P., Marks, D., Link, T., Koenig, G., 2004. Variability of the below canopy thermal structure over snow. *Eos Trans. AGU*, Fall Meet. Suppl., 2004.

Harr, R.D., 1981. Some characteristics and consequences of snowmelt during rainfall in Western Oregon. Journal of Hydrology 53, 277-304.

Helvey, J.D., Fowler, W.B., Klock, G.O., Tiedman, A.R., 1976. Climate and hydrology of the Entiat Experimental Forest watersheds under virgin forest cover. PNW Pacific Northwest Forest Range Experiment Station, General Technical Report, PNW-21, 1-18.

Helvey, J.D., 1980. Effects of a north central Washington wildfire on runoff and sediment production. Water Resources Bulletin 16(4), 627-634.

Leaf, C.F., Alexander, R.R., 1975. Simulating timber yields and hydrologic impacts resulting from timber harvest on subalpine watersheds. USDA Forest Service, Rocky Mountain Forest and Range Experiment Station, Research Paper RM-133.

Link, T., Marks, D., 1999a. Point simulation of seasonal snowcover dynamics beneath Boreal forest canopies. Journal of Geophysical Research, Atmospheres 104(D22), 27841-27858.

Link, T., Marks, D., 1999b. Distributed simulation of snowcover mass- and energy-balance in the Boreal forest. Hydrological Processes 13, 2439-2452.

Loague, K., Heppner, C.S., Mirus, B.B., Ebel, B.A., Ran, Q., Carr, A.E., BeVille, S.H. VanderKwaak, J.E., 2006. Physics-based hydrologic-response simulation: foundation for hydroecology and hydrogeomorphology. Hydrologic Processes 20, 1231-1237.

Marks, D., Winstral, A., Seyfried, M. 2002. Simulation of terrain and forest shelter effects on patterns of snow depostition, snowmelt and runoff over a semi-arid mountain catchment. Hydrologic Processes 16, 3605-3626.

Marks, D., Winstral, A., 2001. Comparison of snow deposition, the snow cover energy balance, and snowmelt at two sites in a semiarid mountain basin. Journal of Hydrometeorology 2, 213-227.

Marks, D., Domingo, Susong, Link, Garen 1999a. A spatially distributed energy balance snowmelt model for application in mountainous basins. Hydrological Processes 13, 1935-1959.

Marks, D., Domingo, J., Frew, J., 1999b. Software tools for hydro-climatic modeling and analysis, Image Processing Workbench (IPW), ARS-USGS Version 2. ARS Technical Bulletin 99-1, Northwest Watershed Research Center, Agricultural Research Service, Boise, Idaho, USA. Electronic document available on the Internet at http://cirque.nwrc.ars.usda.gov/~ipw.

Marks, D., Dozier, J., Davis, R.E., 1992. Climate and energy exchange at the snow surface in the alpine region of the Sierra Nevada, 1, meteorological measurement and monitoring. Water Resources Research 28(11), 3029-3042.

Marks, D., Dozier, J., 1979. A clear-sky longwave radiation model for remote alpine areas. Archiv für Meteorologie, Geophysik und Bioklimatologie, Serie B 27, 159-187.

Mazurkiewicz, A.B., Callery, D.C., McDonnell, J.J., 2006. Physical Controls of snowmelt in the H.J. Andrews Experimental Forest. In the proceedings of the 74th Western Snow Conference, in press.

Mazurkiewicz, A.B., Callery, D.C., McDonnell, J.J., in prep. Physical controls on snowmelt in a rain-on-snow environment. To be submitted to Journal of Hydrology.

McGuire, K.J., 2005. Water residence time and runoff generation in the western Cascades of Oregon. PhD. Dissertation, Department of Forest Engineering, Oregon State University, pp 239.

Meador, W. E., Weaver, W. R., 1980. Two-stream approximations to radiative transfer in planetary atmospheres: a unified description of existing methods and a new improvement. Journal of the Atmospheric Sciences 37, 630-643.

Meiman, J.R. 1987. Influence of forests on snowpack accumulation. Management of subapline forests: Building on 50 yrs of Research. USDA Forest Service, Rocky Mountain Forest and Range Experiment Station. General technical report RM-149.

McClain, M.E., Boyer, E.W., Dent, L., Gergel, S.E., Grimm, N.B., Hart, S.C., Harvey, J.W., Johnston, C.A., Mayorga, E., McDowell, W.H., Pinay, G., 2003. Giogeochemical hot spots and hot moments at the interface of terrestrial and aquatic ecosystems. Ecosystem 6, 301-311.

Mote, P.W., 2003. Trends in snow water equivalent in the Pacific Northwest and their climatic causes. Geophysical Research Letters 30(12), 1-4.

Mote, P.W., Parson, E.A., Hamlet, A.F., Keeton, W.S., Lettenmaier, D, Mantua, N., Miles, E.L., Peterson, D.W., Peterson, D.L., Slaughter, R., Snover, A.K., 2003. Preparing for climatic change: the water, salmon, and forests of the Pacific Northwest. Climatic Change 61, 45-88.

Nolin, A.W., Daly, C., 2006. Mapping “at-risk” snow in the Pacific Northwest, U.S.A. Journal of Hydrometeorology, in press.

Pomeroy, J.W., Toth, B., Granger, R.J., Hedstrom, N.R., Essery, R.L.H., 2003. Variation in surface energetics during snowmelt in a subarctic mountain catchment. Journal of Hydrometeorology 4(4), 702-719.

Ryan, B.C., 1977. A mathematematical model for diagnosis and prediction of surface winds in mountainous terrain. Journal of Applied Meteorology 16 (6), 571-584.

Seibert, J., McDonnell, J.J., 2006. Change detection modeling to assess the effect of forest harvesting and road construction on peak flow. Water Resources Research, in review.

Sensoy, A., Sorman, A. A., Tekeli, A. E., Sorman, A. Ü., Garen, D. C., 2006. Point-scale energy and mass balance snowpack simulations in the upper Karasu basin, Turkey. Hydrological Processes 20, 899-922.

Service, R.F., 2004. As the west goes dry. Science Magazine 303, 1124-1127.

Storck, P., Lettenmaier, D.P., Bolton, S.M., 2002. Measurement of snow interception and canopy effects on snow accumulation and melt in a mountainous maritime climate, Oregon, United States. Water Resources Research 38 (11), 1123, doi:10.1029/2002WR001281.

Susong, D., Marks, D., Garen, D., 1999. Methods for developing time-series climate surfaces to drive topographically distributed energy- and water-balance models. Hydrological Processes 13, 2003-2021.

Troendle, C.A., 1983. Potential for water yield augmentation from forest management in the Rocky Mountain Region. Water Resources Bulletin 19(3), 359-373.

Troendle, C.A., King, R.M., 1985. The effect of timber harvest on the Fool Creek Watershed, 30 years later. Water Resources Research (21), 1915-1922.

Troendle, C.A., King, R.M., 1987. The effect of partial and clearcutting on streamflow at Deadhorse Creek, Colorado. Journal of Hydrology 90, 145-157.

Troendle, C.A., Ruess, J.O., 1997. Effect of clear cutting on snow accumulation and water outflow at Fraser, Colorado. Hydrology and Earth System Sciences 1 (2), 325-332.

Weiler, M., McDonnell, J., 2004. Virtual Experiments: a new approach for improving process conceptualization in hillslope hydrology. Journal of Hydrology 285, 3-18.

Winkler, R.D., Spittlehouse, D.L., Golding, D.L., 2005. Measured differences in snow accumulation and melt among clearcut, juvenile, and mature forests in southern British Columbia. Hydrological Processes 19, 51-62.

Winstral, A., Marks, D., 2002. Simulating wind fields and snow redistribution using terrain-based parameters to model snow accumulation and melt over a semi-arid mountain catchment. Hydrological Processes 16, 3585-3603.

Woodsmith, R.D., Vache, K.B., McDonnell, J.J., Helvey, J.D. 2004. Entiat Experimental Forest: Catchment-scale runoff data before and after a 1970 wildfire. Water Resources Research 49, W11701, doi 10.1029/2004WRR003296.

Van Havern, B.P., 1998, Reevaluation of the Wagon Wheel Gap Forest Watershed Experiment. Forest Science 4(1), 208-214.

van Heesjwick, M., Kimball, J., Marks, D. 1996. Simulation of water available for runoff in clearcut forest openings during rain-on-snow events in the western Cascade Range of Oregon and Washington. Water Resources Investigations Report 95-4219 US Geological Survey, Tacoma, Washington, 67 pg.

VanShaar, J.R., Haddeland, I., Lettenmaier, D.P., 2002. Effects of land-cover changes on the hydrological response of interior Columbia basin forested catchments. Hydrological Processes 16, 2499-2520.

Table 3.1 Meteorological measurements

Parameter	*Sensor*	*Sampling Interval*	*Precision*	*Instrument Heat (above soil surface)*
Wind speed	Onset	30 min.	0.01 m/s	2.5 m
Air Temperature	Onset	30 min.	0.01°C	1.5 m
Relative Humidity	Onset	30 min.	0.01	1.5 m
Shortwave Radiation	Li-Cor 200(0.4 to 1.1µm)	15 min.	0.01 w/m^2	2.5 m
SWE	Schavetiz Ultrastable 60	15 min.	0.1 mm	

Table 3.2 Station characteristics and measurements

	Elevation (m)	***Site Description***	***Measurements***
Weir Met	872	Mature Forest Opening	Air Temp, Wind Speed, Snow Depth
Waterfall	1097	Open	Air Temp, RH
Lower Pillow	1211	Open	Air Temp, SWE, Snow Depth, Solar Radiation
510 Rd	1270	Open	RH, Air Temp, Wind Speed, Wind Direction
Upper Pillow	1536	Young Forest Opening	Air Temp, SWE, Snow Depth
Frog Rx	1697	Open	Air Temp, RH, Wind Speed, Wind Direction

Table 3.3 Vegetation parameters

Vegetation type	***tau (t)***	***Mu***
Dense successional forest	0.44	0.033
Low density succesional forest/mature	0.30	0.025
Open	1	1

Table 3.4 Precipitation type

Dew Point (D_t)	*% snow*	*kg/m^2*
D_t <-5	100	100
-5 <= D_t <-3	100	100
-3 <= D_t <-1.5	100	150
-1.5 <= D_t <-0.5	100	175
-0.5 <= D_t < 0	75	200
0 <= D_t < 0.5	25	250
0.5 <= D_t	0	1000

Table 3.5 Model run descriptions

Model Run	***Description***	***Effected forcing data***
2006	Mixed vegetation cover	
Veg-Free	Vegetation corrections removed	Precipitation, solar radiation, thermal wind speed
100% Veg	Apply a	Precipitation, thermal and solar radiation, wind speed
2020	Increase of temperature 2.7 C	Air temperature, vapor pressure, thermal radiation
2040	Increase of temperature 4.1 C	Air temperature, vapor pressure, thermal radiation

Table 3.6 Weighted EB components for WAR, by percentage and mm/year

	2006			2020			2040			Veg-Free			100% Veg		
	Upper	Lower	Weir	Upper	Lower	Weir	Upper	Lower	Weir	Upper	Lower	Weir	Upper	Lower	Weir
% Rn	81	93	89	73	75	91	64	57	84	82	85	90	84	81	85
% H	17	3	4	22	5	4	22	8	8	17	13	7	12	12	9
%Lve	2	2	2	3	2	1	6	5	4	1	1	1	3	4	1
%Grnd	0	2	2	0	3	1	1	6	2	0	1	1	1	3	2
% Adv	0	1	3	2	14	3	7	25	2	0	0	2	0	0	2
Rn (mm/yr)	648	596	443	569	460	430	485	294	393	653	563	452	641	519	422
H (mm/yr)	133	19	21	167	31	20	167	41	37	134	84	34	92	77	46
Lve (mm/yr)	14	10	11	25	15	3	50	26	19	12	5	3	26	28	6
Grnd (mm/yr)	2	13	8	3	17	6	7	29	8	2	6	4	6	18	10
Adv (mm/yr)	0	5	17	12	89	15	55	130	10	0	1	11	1	2	11

Table 3.7 Peak SWE for each snow pillow and overall basin.

	2006	*SWE (mm)*	*2020*	*SWE (mm)*	*2040*	*SWE (mm)*	*Veg Free*	*SWE (mm)*	*100% Veg*	*SWE (mm)*
Lower	20-Mar	539	8-Feb	202	2-Feb	202	20-Mar	610	19-Apr	607
Upper	20-Mar	743	20-Mar	659	20-Mar	504	21-Mar	746	18-Apr	747
Basin	21-Mar	246	20-Mar	158	4-Feb	94	20-Mar	237	19-Apr	256

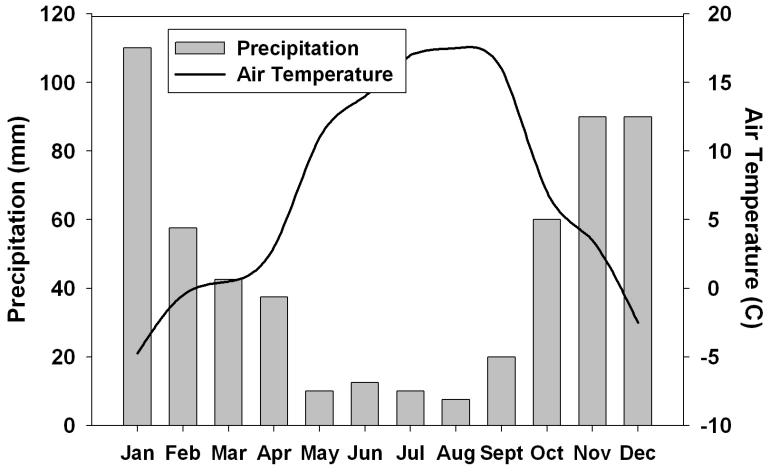

Figure 3.1 Climograph adapted from Helvey et. al. (1976) for precipitation records 1961 to 1970 and air temperature, 1966 to 1970.

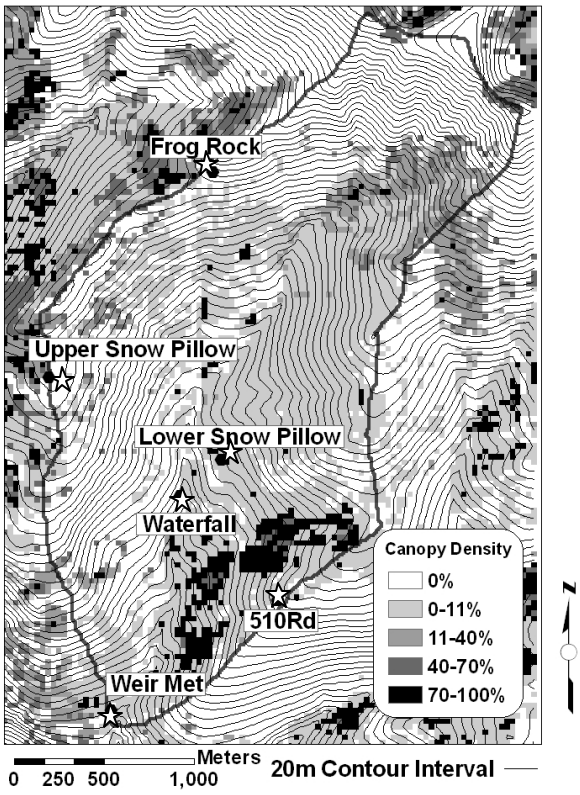

Figure 3.2 Meteorological stations and canopy density within the Burns watershed.

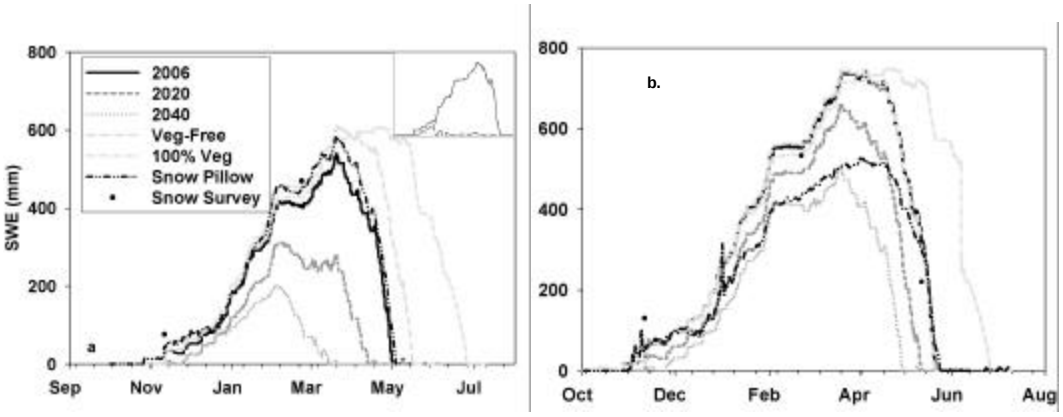

Figure 3.3. Lower Snow Pillow (a) with inset of temperature index model and Upper Snow Pillow (b) measured and modeled SWE.

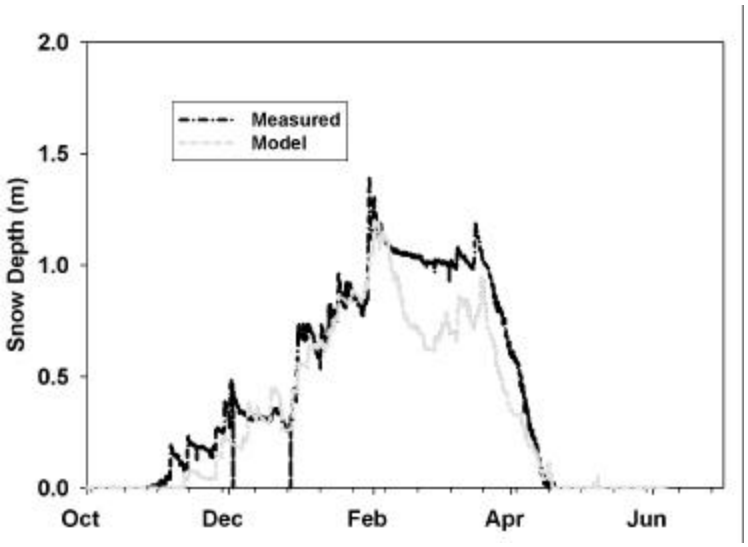

Figure 3.4 Weir meteorological station measured and modeled snow depth for water year 2006.

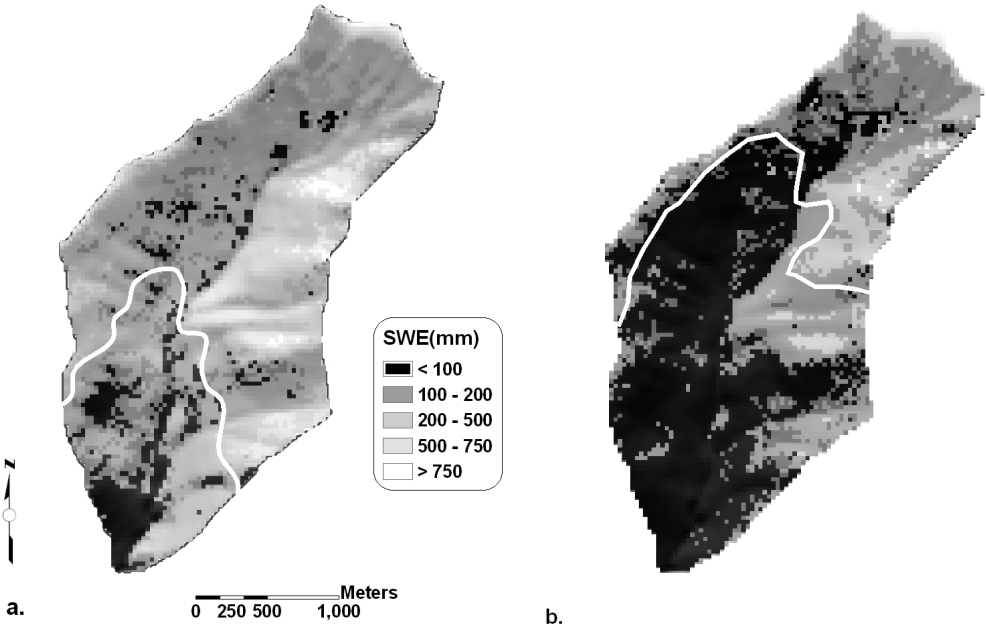

Figure 3.5 Modeled SWE in the Burns basin. The white line depicts the estimated snow line from oblique basin photographs for April 25 (a) and May 9 2006 (b.).

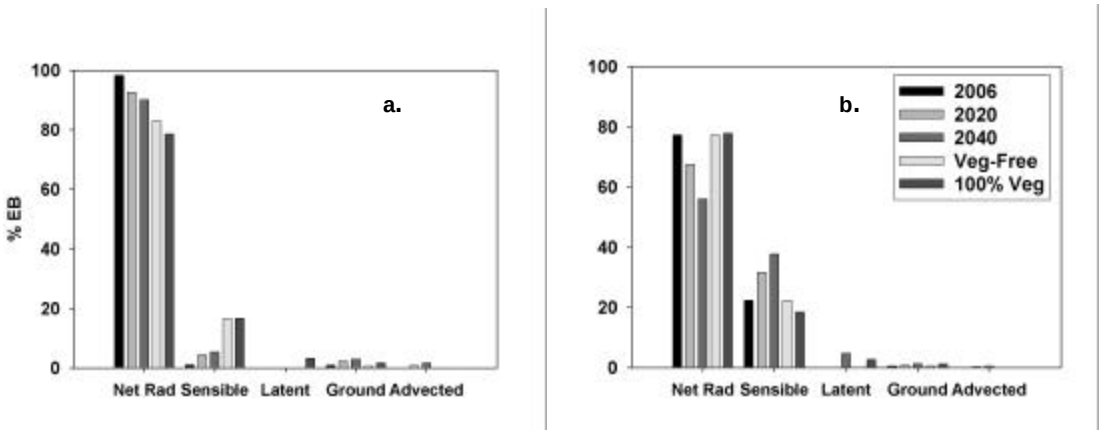

Figure 3.6 Annual energy balance budget for melt at the Lower (a.) and Upper (b.) Snow Pillow.

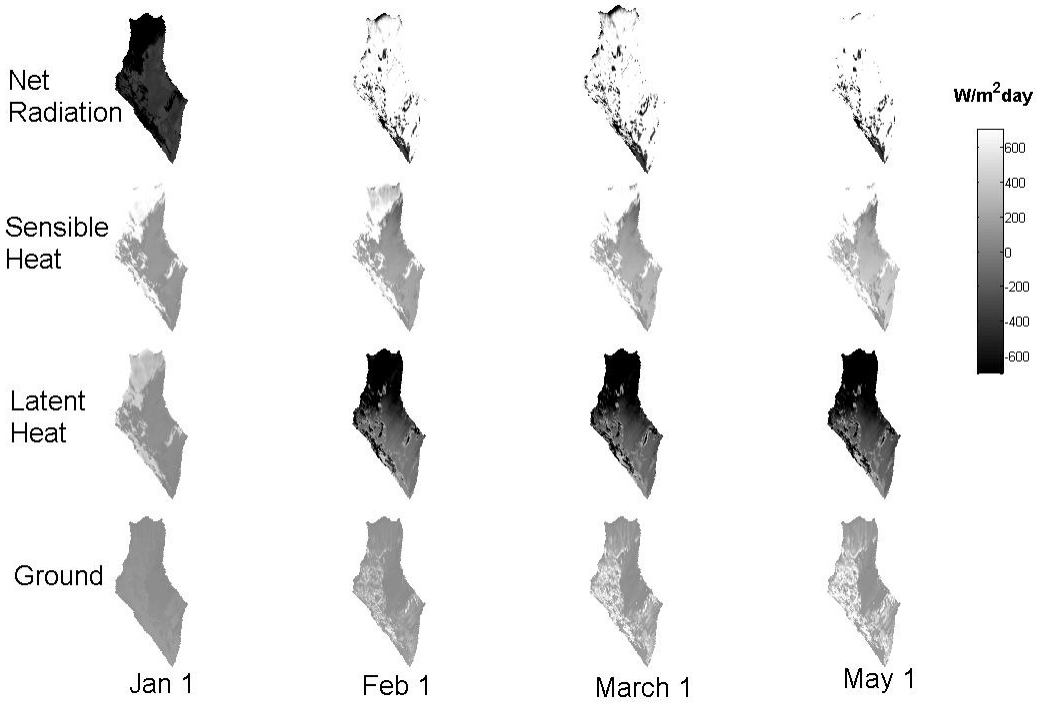

Figure 3.7. Daily energy balance components for WY 2006 simulation

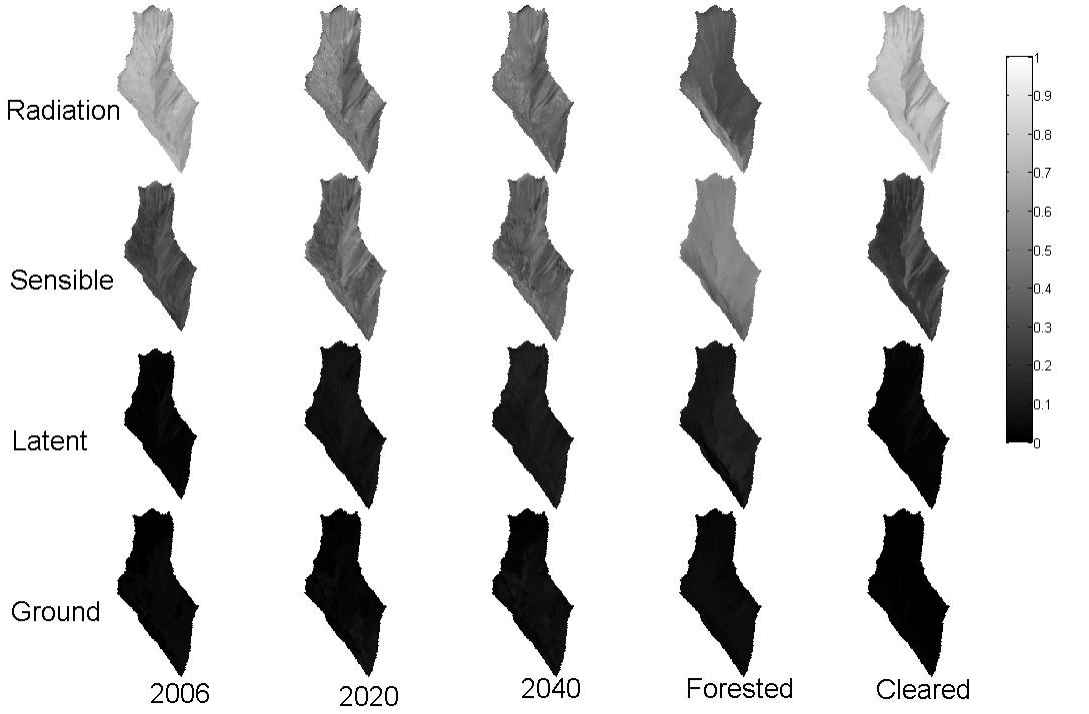

Figure 3.8 Weighted EB components as a percent of WAR

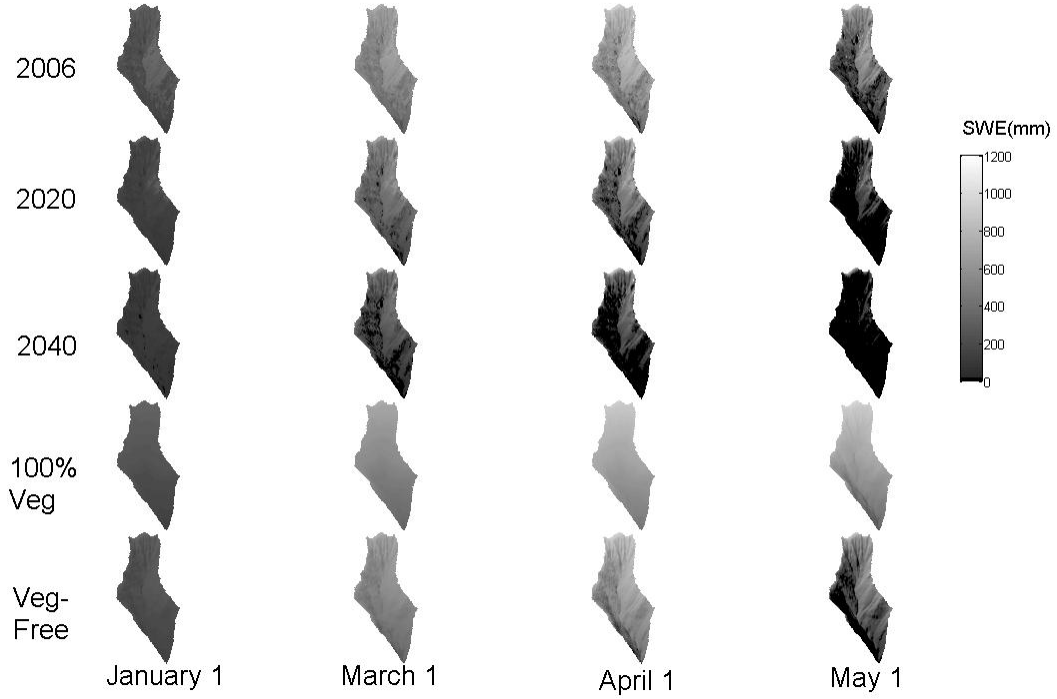

Figure 3.9 Distributed SWE maps for each of the model runs.

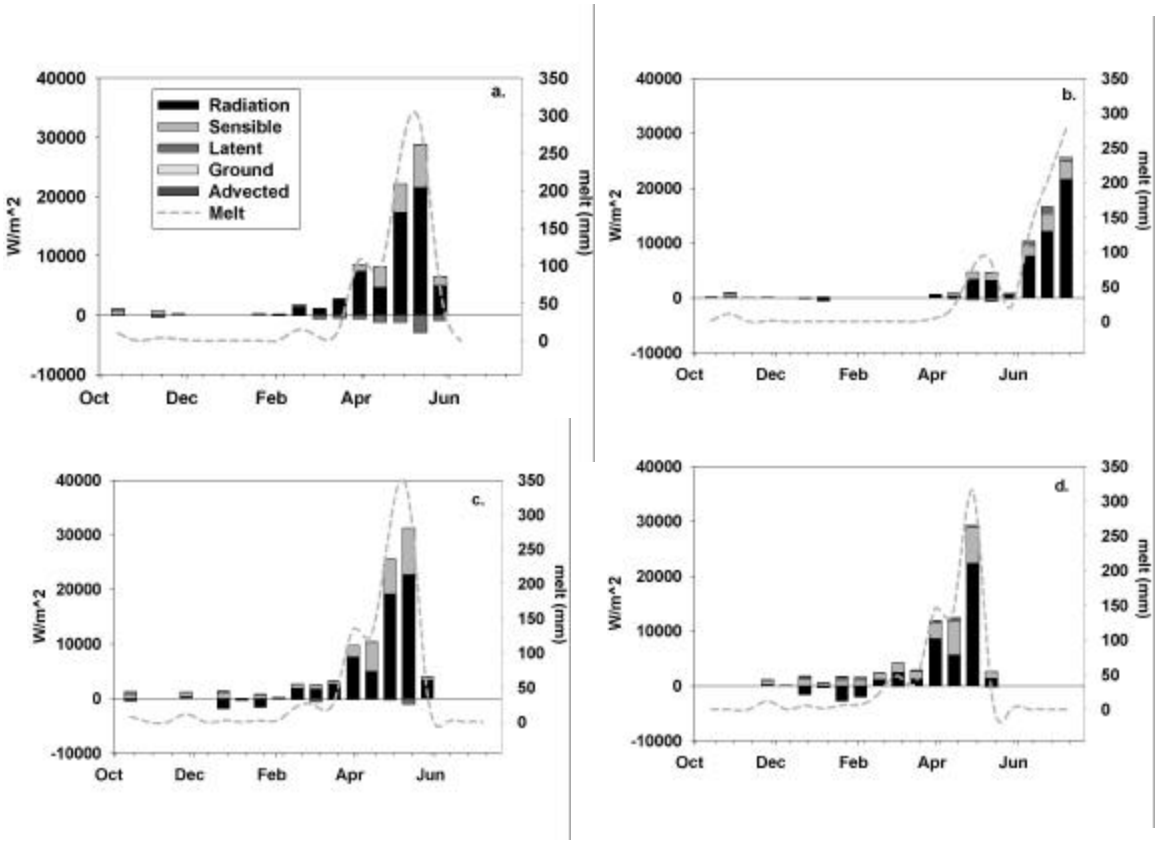

Figure 3.10 Upper Snow Pillow biweekly EB and melt – 2006 (a.), 100% Veg (b), 2020 (c), and 2040 (d).

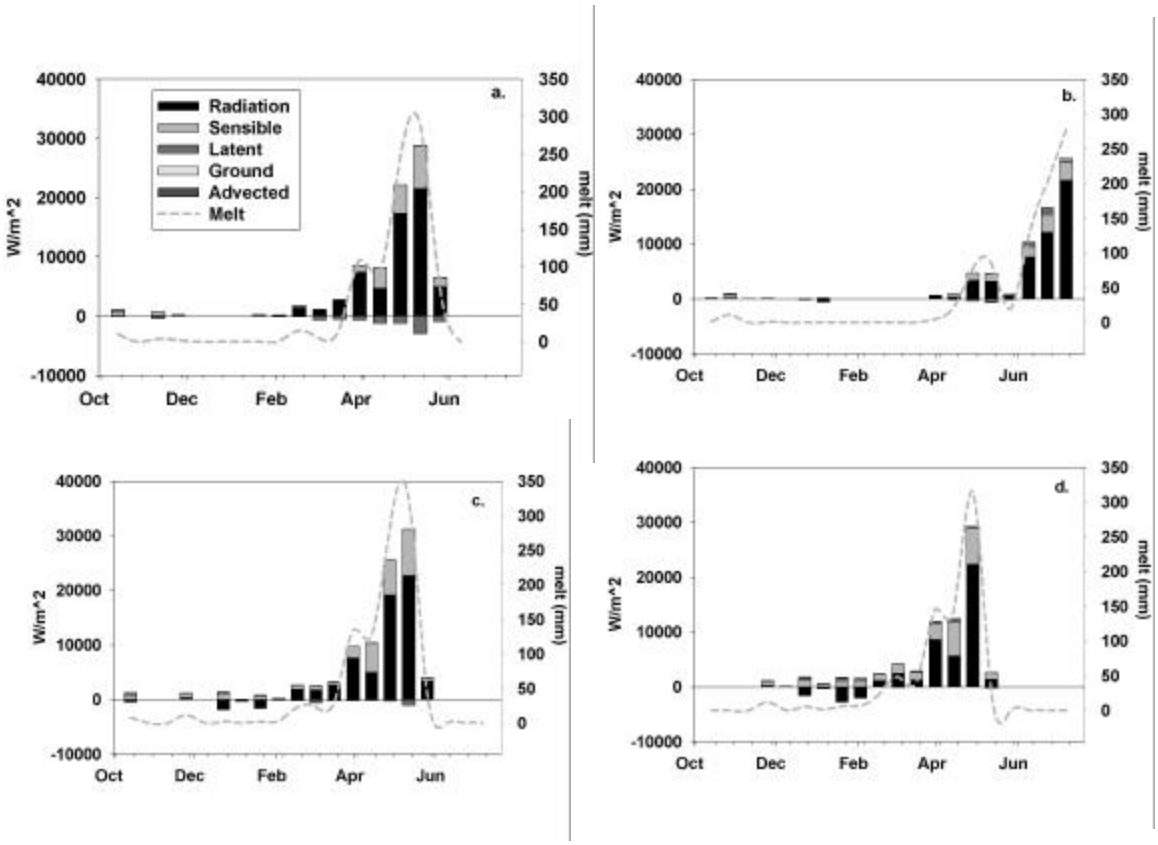

Figure 3.11 Lower Snow Pillow bi-weekly EB and melt – 2006 (a.), 100% Veg (b), 2020 (c), and 2040 (d).

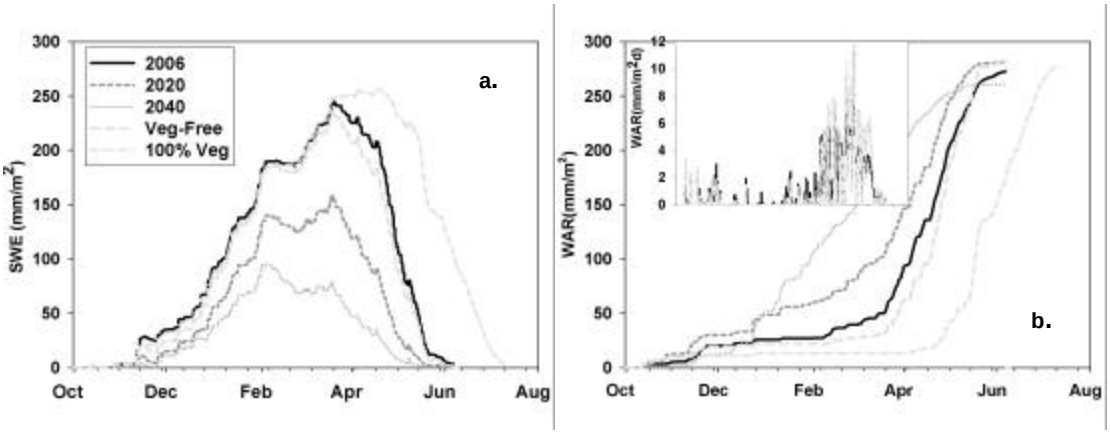

Figure 3.12 Annual Basin SWE (a.) and annual basin WAR (b.) with daily basin WAR for vegetation free and 2006 model runs inset.

4 CONCLUSIONS

4.1 CONCLUSIONS

This thesis has presented results from two investigations which successfully apply a physically-based model in two different climate and snow regimes of the Pacific Northwest. In both modeling studies we have shown that net radiation is the dominant EB component snowmelt. The temporal and spatial variability of EB components were highly dependent on topographic position and length of the snow season.

The results in chapter 1 shed light on melt regime which has been generalized to be turbulent exchange dominated. Our investigation into the controls of the snowmelt energy balance provides new insight into the dominant melt processes in the HJA. We found that net radiation dominated the snowmelt energy balance over the period 1996-2003 at our three measurements sites: UPLMET 80%, VANMET 55%, and at CENMET 49%. Annual variability in the EB components reflected the time duration of the snowpack (snow covered period). A snowpack which lingered into the spring resulted in higher amounts of radiation as a percent of total EB components. Melt seasons with more transient snow resulted in higher percentages of turbulent exchange contributing the EB. Ground heat flux integrated over the modeling period proved to be a large contributor to the EB.

In chapter 2 we have shown that radiation is an important component of the EB in environmental change scenarios for the semi-arid Eastern Washington Cascades. Radiation inputs accounted for up to 98% of the energy creating WAR in WY 2006. This large contribution of net radiation energy dominated the EB for melt in climate change and land cover change modeling scenarios. Forested model runs also indicated

high radiation inputs in creating WAR due to longer snow seasons which received early summer solar insolation. The annual percentage of sensible heat contributions increased 4-5% during the shorter snow seasons in the 2020 and 2040 model simulations. Sensible heat exchanges were positive throughout the winter. These fluxes caused melt throughout the winter. Removal of the forest canopy increased turbulent fluxes in the basin which had vegetation influences. The percent of WAR attributed to sensible heat flux at the lower snow pillow increased by 10% due to canopy removal.

4.2 Future work

The continued application of physically-based snow energy models highlights the need for support of developed climate and research networks such as SNOTEL, LTER, and RAWS to continue measuring parameters and to expand the number and types of measurement. Without these networks, meso-scale modeling routines have little basis to ensure accurate predictions. Increased attention and support directed towards these networks will improve the future abilities to identify and quantify variations in the snow regime.

The growing use of models to generate scenarios of environmental change effects requires the refinement of parameterization in order to reduce uncertainty of model outputs. Intensive snow hydrology field studies, such as U.S.A.C.E. (1956), need to be repeated with new measurement technology. The increase in our knowledge and tools require intensive snow hydrology studies to help parameterize the complex physically-based models which have been developed. The physically-based models will be of little use if we cannot apply them appropriately in complex

mountainous terrain. Measurements of vegetation thermal radiation, albedo decay, ground heat flux, and advective heat transfer will help to develop parameters across a wide range of vegetation types and conditions. In our findings, sensible heat exchange was the second most important EB component. This EB component has been proven to be significant during major storm events with high wind speeds. However, there are few measurements to ensure the modeling approaches that we have taken are valid. Continued measurements of these exchanges will help to validate our models and provide additional insight to the snowmelt regimes of the PNW.

4.3 REFERENCES

U.S.A.C.E. (U.S. Army Corps of Engineers), 1956. Snow Hydrology. U.S. Army Corps pf Engineers, Portland, Oregon, 437 pp.

5 BIBLIOGRAPHY

Berris, S., Harr, R.D., 1987. Comparative snow snow accumulation and melt during rainfall in forested and clear-cut plots in the western Cascades of Oregon. Water Resources Research 23, 135-142.

Blöschl, G., 1999. Scaling issues in snow hydrology. Hydrological Processes 13, 2149-2175.

Chelan County Conservation District (CCCD), 2004. Entiat Water Resource Inventory Area(WRIA) 46 Watershed Management Plan. Electronic document available on Internet at http://www.chelancd.org/WRIA46_Plan.htm

Climate Impacts Group (CIG), 2004. Overview of climate change impacts in the U.S. Pacific Northwest. University of Washington, Seattle, WA. Electronic document available on Internet at www.cses.washington/edu/cig.

Christensen, N.S., Wood, A.W., Voisin, N. Lettenmaier, D.P., Palmer, R.N., 2004. The Effects of Climate Change on the Hydrology and Water Resources of the Colorado River Basin, Climatic Change 62 (1), 337-363.

Daly, C., Nelison, R.D. Phillips, D.L., 1994. A statistical topographic model for mapping climatological precipitation over mountainous terrain. Journal of Applied Meteorology 33, 140-158.

Frew, J., 1990. The Image Processing Workbench. PhD Thesis, Department of Geography, University of California, Santa Barbara, CA, pp. 382.

Garen, D. Marks, D., 2005. Spatially distributed energy balance snowmelt modeling in a mountainous river basin: Estimation of meteorological inputs and verification of model results. Journal of Hydrology 315, 126-153.

Garen, D.C., Johnson, G.L., Hanson, C.L., 1994. Mean areal precipitation for daily hydrologic modeling in mountainous regions. Water Resources Bulletin 30(3), 481-491.

Gary, H.L., 1974. Snow accumulation and snowmelt as influenced by a small clearing in a Lodgepole Pine forest. Water Resources Research 10(2), 348-353.

Golding, D.L., Swanson, R.H., 1986. Snow distribution patterns in clearing and adjacent forest. Water Resources Research 22(13), 1931-1940.

Greenland, David. 1994. The Pacific Northwest regional context of the climate of the H.J. Andrews Experimental Forest. Northwest Science. 69(2), 81-96.

Hardy, J.P., Marks, D., Link, T., Koenig, G., 2004. Variability of the below canopy thermal structure over snow. *Eos Trans. AGU*, Fall Meet. Suppl., 2004.

Hardy, J., Melloh, R., Robinson, P., Jordan, R., 2000. Incorporating effects of forest litter in a snow process model. Hydrological Processes 14, 3227-3237.

Harr, R.D., Berris, S.N., 1983. Snow accumulation and subsequent melt during rainfall in forested and clearcut plots in Western Oregon. In the Proceedings of the 51st Western Snow Conference, 38-44.

Harr, R.D., 1981. Some characteristics and consequences of snowmelt during rainfall in Western Oregon. Journal of Hydrology 53, 277-304.

Helvey, J.D., Fowler, W.B., Klock, G.O., Tiedman, A.R., 1976. Climate and hydrology of the Entiat Experimental Forest watersheds under virgin forest cover. PNW Pacific Northwest Forest Range Experiment Station, General Technical Report, PNW-21, 1-18.

Helvey, J.D., 1980. Effects of a north central Washington wildfire on runoff and sediment production. Water Resources Bulletin 16(4), 627-634.

Johnson, J.B., Schaefer, G.L., 2002. The influence of thermal, hydrologic, and snow deformation mechanisms on snow water equivalent pressure sensor accuracy. Hydrological Processes 16, 3529-3542.

Jones, J.A., Swanson, F.J. 2001. Hydrologic inferences from comparisons among small basin experiments. Hydrological Processes 15, 2363-2366.

Jones, J. A.., Grant G.E., 1996. Peak flow responses to clear-cutting and roads in small and large basins, western Cascades, Oregon. Water Resources Research 32, 959-974.

Leaf, C.F., Alexander, R.R., 1975. Simulating timber yields and hydrologic impacts resulting from timber harvest on subalpine watersheds. USDA Forest Service, Rocky Mountain Forest and Range Experiment Station, Research Paper RM-133.

Link, T., Marks, D., 1999. Point simulation of seasonal snowcover dynamics beneath Boreal forest canopies. Journal of Geophysical Research, Atmospheres 104(D22), 27841-27858.

Link, T., Marks, D., 1999. Distributed simulation of snowcover mass- and energy-balance in the Boreal forest. Hydrological Processes 13, 2439-2452.

Loague, K., Heppner, C.S., Mirus, B.B., Ebel, B.A., Ran, Q., Carr, A.E., BeVille, S.H. VanderKwaak, J.E., 2006. Physics-based hydrologic-response simulation: foundation for hydroecology and hydrogeomorphology. Hydrologic Processes 20, 1231-1237.

Male, D.H., Gray, D.M., 1981. Snowcover ablation and runoff. In: Gray, D.H., Male, D.M. (Eds.), Handbook of Snow, Permagon Press, Willowdale, Canada, pp 360-430.

Marks, D., Link, T., Winstral, A., Garen, D., 2001. Simulating snowmelt processes during rain-on-snow over a semi-arid mountain basin. Annals of Glaciology 32, 195-202.

Marks, D., Winstral, A., Seyfried, M. 2002. Simulation of terrain and forest shelter effects on patterns of snow depostition, snowmelt and runoff over a semi-arid mountain catchment. Hydrologic Processes 16, 3605-3626.

Marks, D., Winstral, A., 2001. Comparison of snow deposition, the snow cover energy balance, and snowmelt at two sites in a semiarid mountain basin. Journal of Hydrometeorology 2, 213-227.

Marks, D., Domingo, Susong, Link, Garen 1999a. A spatially distributed energy balance snowmelt model for application in mountainous basins. Hydrological Processes 13, 1935-1959.

Marks, D., Domingo, J., Frew, J., 1999b. Software tools for hydro-climatic modeling and analysis, Image Processing Workbench (IPW), ARS-USGS Version 2. ARS Technical Bulletin 99-1, Northwest Watershed Research Center, Agricultural Research Service, Boise, Idaho, USA. Electronic document available on the Internet at http://cirque.nwrc.ars.usda.gov/~ipw.

Marks, D., Dozier, J., Davis, R.E., 1992. Climate and energy exchange at the snow surface in the alpine region of the Sierra Nevada, 1, meteorological measurement and monitoring. Water Resources Research 28(11), 3029-3042.

Marks, D., Dozier, J., 1979. A clear-sky longwave radiation model for remote alpine areas. Archiv für Meteorologie, Geophysik und Bioklimatologie, Serie B 27, 159-187.

Mazurkiewicz, A.B., Callery, D.C., McDonnell, J.J., 2006. Physical Controls of snowmelt in the H.J. Andrews Experimental Forest. In the proceedings of the 74th Western Snow Conference, in press.

Mazurkiewicz, A.B., Callery, D.C., McDonnell, J.J., in prep. Physical controls on snowmelt in a rain-on-snow environment. To be submitted to Journal of Hydrology.

McGuire, K.J., 2005. Water residence time and runoff generation in the western Cascades of Oregon. PhD. Dissertation, Department of Forest Engineering, Oregon State University, pp 239.

Meador, W. E., and W. R. Weaver, 1980. Two-stream approximations to radiative transfer in planetary atmospheres: a unified description of existing methods and a new improvement. Journal of the Atmospheric Sciences 37, 630-643.

Meiman, J.R. 1987. Influence of forests on snowpack accumulation. Management of subapline forests: Building on 50 yrs of Research. USDA Forest Service, Rocky Mountain Forest and Range Experiment Station. General technical report RM-149.

McClain, M.E., Boyer, E.W., Dent, L., Gergel, S.E., Grimm, N.B., Hart, S.C., Harvey, J.W., Johnston, C.A., Mayorga, E., McDowell, W.H., Pinay, G., 2003. Giogeochemical hot spots and hot moments at the interface of terrestrial and aquatic ecosystems. Ecosystem 6, 301-311.

Mote, P.W., 2003. Trends in snow water equivalent in the Pacific Northwest and their climatic causes. Geophysical Research Letters 30(12), 1-4.

Mote, P.W., Parson, E.A., Hamlet, A.F., Keeton, W.S., Lettenmaier, D, Mantua, N., Miles, E.L., Peterson, D.W., Peterson, D.L., Slaughter, R., Snover, AK., 2003. Preparing for climatic change: the water, salmon, and forests of the Pacific Northwest. Climatic Change 61, 45-88.

Nolin, A.W., Daly, C., 2006. Mapping "at-risk" snow in the Pacific Northwest, U.S.A. Journal of Hydrometeorology, in press.

Pomeroy, J.W., Toth, B., Granger, R.J., Hedstrom, N.R., Essery, R.L.H., 2003. Variation in surface energetics during snowmelt in a subarctic mountain catchment. Journal of Hydrometeorology 4(4), 702-719.

Ryan, B.C., 1977. A mathematematical model for diagnosis and prediction of surface winds in mountainous terrain. Journal of Applied Meteorology 16 (6), 571-584.

Seibert, J., McDonnell, J.J., 2006. Change detection modeling to assess the effect of forest harvesting and road construction on peak flow. Water Resources Research, in review.

Sensoy, A., Sorman, A. A., Tekeli, A. E., Sorman, A. Ü., Garen, D. C., 2006. Point-scale energy and mass balance snowpack simulations in the upper Karasu basin, Turkey. Hydrological Processes 20, 899-922**.**

Serreze, M.C., Clark, M.P., Armstrong, R.L., McGinnis, D.A., Pulwarty, R.S., 1999. Characteristics of the western United States snowpack from snowpack telemetry (SNOTEL) data. Water Resources Research 35(7), 2145-2160.

Service, R.F., 2004. As the west goes dry. Science Magazine 303, 1124-1127.

Storck, P., Lettenmaier, D.P., Bolton, S.M., 2002. Measurement of snow interception and canopy effects on snow accumulation and melt in a mountainous maritime climate, Oregon, United States. Water Resources Research 38 (11), 1123, doi:10.1029/2002WR001281.

Susong, D., Marks, D., Garen, D., 1999. Methods for developing time-series climate surfaces to drive topographically distributed energy- and water-balance models. Hydrological Processes 13, 2003-2021.

Troendle, C.A., 1983. Potential for water yield augmentation from forest management in the Rocky Mountain Region. Water Resources Bulletin 19(3), 359-373.

Troendle, C.A., King, R.M., 1985. The effect of timber harvest on the Fool Creek Watershed, 30 years later. Water Resources Research (21), 1915-1922.

Troendle, C.A., King, R.M., 1987. The effect of partial and clearcutting on streamflow at Deadhorse Creek, Colorado. Journal of Hydrology 90, 145-157.

Troendle, C.A., Ruess, J.O., 1997. Effect of clear cutting on snow accumulation and water outflow at Fraser, Colorado. Hydrology and Earth System Sciences 1 (2), 325-332.

U.S.A.C.E. (U.S. Army Corps of Engineers), 1956. Snow Hydrology. U.S. Army Corps pf Engineers, Portland, Oregon, 437 pp.

Weiler, M., McDonnell, J., 2004. Virtual Experiments: a new approach for improving process conceptualization in hillslope hydrology. Journal of Hydrology 285, 3-18.

Winkler, R.D., Spittlehouse, D.L., Golding, D.L., 2005. Measured differences in snow accumulation and melt among clearcut, juvenile, and mature forests in southern British Columbia. Hydrological Processes 19, 51-62.

Winstral, A., Marks, D., 2002. Simulating wind fields and snow redistribution using terrain-based parameters to model snow accumulation and melt over a semi-arid mountain catchment. Hydrological Processes 16, 3585-3603.

Wondzell, S.M., King, J.G., 2003. Postfire erosional proceses in the Pacific Northwest and Rocky Mountain regions. Forest Ecology and Management 178: 75-87.

Woodsmith, R.D., Vache, K.B., McDonnell, J.J., Helvey, J.D. 2004. Entiat Experimental Forest: Catchment-scale runoff data before and after a 1970 wildfire. Water Resources Research 49, W11701, doi 10.1029/2004WRR003296.

Van Havern, B.P., 1998, Reevaluation of the Wagon Wheel Gap Forest Watershed Experiment. Forest Science 4(1), 208-214.

van Heesjwick, M., Kimball, J., Marks, D. 1996. Simulation of water available for runoff in clearcut forest openings during rain-on-snow events in the western Cascade Range of Oregon and Washington. Water Resources Investigations Report 95-4219 US Geological Survey, Tacoma, Washington, 67 pg.

VanShaar, J.R., Haddeland, I., Lettenmaier, D.P., 2002. Effects of land-cover changes on the hydrological response of interior Columbia basin forested catchments. Hydrological Processes 16, 2499-2520.